EFFECT OF METAL OXIDE SUPPORTS ON ACTIVE-CU FOR CO_x HYDROGENATION TO METHANOL

EFFECT OF METAL OXIDE SUPPORTS ON ACTIVE-CU FOR CO_x HYDROGENATION TO METHANOL

By

Adarsh PATIL

in partial fulfilment of the requirements for the degree of
Master of Science
in Chemical Engineering,

at the Delft university of Technology,
to be defended publicly on Tuesday April 14, 2020 at 09:00 AM.

Supervisor:	Prof. dr. A. Urakawa
Thesis committee:	Prof. dr. B. Dam,
	Prof. dr. W. de Jong.

An experiment is a question which science poses to Nature and a measurement is the recording of Nature's answer.

Max Planck

CONTENTS

ABSTRACT

Increasing tensions over global warming, talks about a sustainable future and a huge imbalance in closure of the carbon cycle indicate a response for developing efficient conversion of CO_2 and syngas obtained from renewable sources. Thermochemical conversion of carbon oxides (CO and CO_2) in combination with hydrogen to produce methanol in the presence of catalyst provides a pathway to close this carbon cycle. Steady state activity tests were carried out in a small integral reactor for methanol synthesis from a mixture of either CO/H_2 or CO_2/H_2. The temperature was varied from 200 to 300°C, while the total pressure was held constant for CO/H_2 at 85 bar and CO_2/H_2 at 60 bar keeping stoichiometric flow of hydrogen at GHSV of 24,000 hr^{-1}.

Four different metal oxides namely ZnO, ZrO_2, MgO and CeO_2 were investigated for support effects on active Cu along with different combinations among them while keeping commercial catalyst as the benchmark. Catalysts were prepared using urea hydrolysis method. It was found that ZrO_2 and MgO show higher selectivity however the latter does not exhibit comparable conversion as the commercial catalyst for CO_2 hydrogenation. Detailed GHSV study for Cu-ZrO_2 paint a completely different picture showing higher methanol selectivity (64%) with increasing space velocity (at GHSV of 32,000 hr^{-1}). In case of CO hydrogenation, commercial catalyst performs the best, albeit displaying signs of carbon deposition at higher temperature (280°, 300°C). This situation is circumvented by employing ZnO/MgO combination as a support.

Cu-CeO_2 exhibited characteristics of an excellent water gas shift catalyst. This led to a novel configuration of mixed bed consisting of Cu-CeO_2 with commercial catalyst. Results indicate that this combination improves the methanol yield by atleast 30% as compared to commercial catalyst at a high GHSV of 24,000 hr^{-1}.

Keywords: Copper, CO_2 hydrogenation, GHSV (Gas hourly space velocity), Methanol, Urea hydrolysis.

1

INTRODUCTION

1.1. CONTEXT

THere is a growing consensus about the greenhouse potential of carbon dioxide and its causal link between global warming. Atmospheric CO_2 levels show an increasing trend over the past few years and are currently the highest during post-industrial revolution era[1]. This has led to establishment of several international institutions such as Intergovernmental Panel on Climate Change (IPCC) and the United Nations Framework Convention on Climate Change. Although CO_2 is the main culprit for this situation, humanity relies heavily on technologies powered by fossil fuels further aggravating the issue. Despite shifting our dependence from fossil fuels to renewables for energy consumption, reliance of mankind on carbon as an element is huge. This is evident by the share of petrochemical industry in everyday products. Because of the incomplete carbon cycle, it may run out of its most important feedstock. Increasing efforts of replacing coal with biomass as a source of syngas, and converting CO_2 to methanol will help in contributing to overall sustainable development.

1.2. BACKGROUND

METHANOL is a versatile chemical compound. It is widely used as a raw material to produce a wide variety of chemicals based on fossil fuels such as Ethylene or Propylene in the Methanol to Olefin (MTO) process[2]. It has also been widely suggested to be used as a fuel in the Methanol economy proposed by Steinberg and Olah, wherein methanol and dimethyl ether replace conventional fossil fuels as fuel source, and raw materials for producing synthetic hydrocarbons. Methanol can be used in Internal Combustion Engines (ICEs) either in its pure liquid state or as a blend with gasoline. These features make it a stand-out alternative which can be easily scaled up in production and possesses less safety issues for transportation and storage when compared to hydrogen as a fuel[3]. Another advantage of producing methanol is that its synthesis is already done on a large scale, thereby circumventing the need of scaling up the process in terms of maturity and technical knowledge.

1

1.2.1. METHANOL FROM SYNGAS

The traditional method of producing Methanol is upgrading synthesis gas (also known as syngas) via hydrogenation. Synthesis gas can be produced from a wide variety of sources such as natural gas, shale gas, coal and biomass. Methanol from syngas involves the following reactions:

$$CO_{(g)} + 2H_{2(g)} \leftrightarrow CH_3OH_{(g)} \qquad \Delta H_{298} = -90.5 kJ/mol \tag{1.1}$$

$$CO_{2(g)} + 3H_{2(g)} \leftrightarrow CH_3OH_{(g)} + H_2O_{(g)} \qquad \Delta H_{298} = -49.4 kJ/mol \tag{1.2}$$

$$CO_{2(g)} + H_{2(g)} \leftrightarrow CO_{(g)} + H_2O_{(g)} \qquad \Delta H_{298} = 41.1 kJ/mol \tag{1.3}$$

Syngas is converted to methanol in the operating range of 250-300°C, 50-100 bar with SN (Stoichiometric number) ranging from 2-2.1 (30% of the carbon in syngas is composed of CO_2 [4]) over commercial catalyst ($Cu/ZnO/Al_2O_3$)[5].

$$SN = \frac{y_{H_2} - y_{CO_2}}{y_{CO} + y_{CO_2}} \tag{1.4}$$

Here, y denotes partial pressure or mole fractions of the gaseous components according to the subscript notation. The desired SN (stoichiometric number) in the feed is equal to 2. SN > 2 indicates an excess of hydrogen while SN < 2 indicates carbon rich feed mixture.
Reactions 1.1 and 1.2 are highly exothermic in nature and involve reduction in number of gases towards the product side. Hence, according to Le Chatelier's principle, high pressure and low temperature favour higher conversion. However, due to kinetic limitation at lower temperatures, the reaction cannot be performed at this condition due to low single pass conversion.

1.2.2. METHANOL FROM CO_2

Although CCS (Carbon Capture and Storage) provides a solution for capturing CO_2 from the atmosphere and storing it underground or some other facilities, it poses an inherent risk of a possible leak in the future and treats CO_2 as waste instead of producing valuable chemicals. CO_2 hydrogenation to methanol goes a step further than CCS. It produces methanol which acts as feedstock for other products, not only adding value to the CO_2 captured but consequently closes the carbon cycle. Moreover, production of methanol from CO_2 has attracted attention recently as it provides an alternative for industrial syngas hydrogenation process due to its reported high reaction rates. Besides this, the process has potential of being highly sustainable, given the required hydrogen is produced via electro-chemical splitting of water using electricity from renewable sources such as wind and solar.

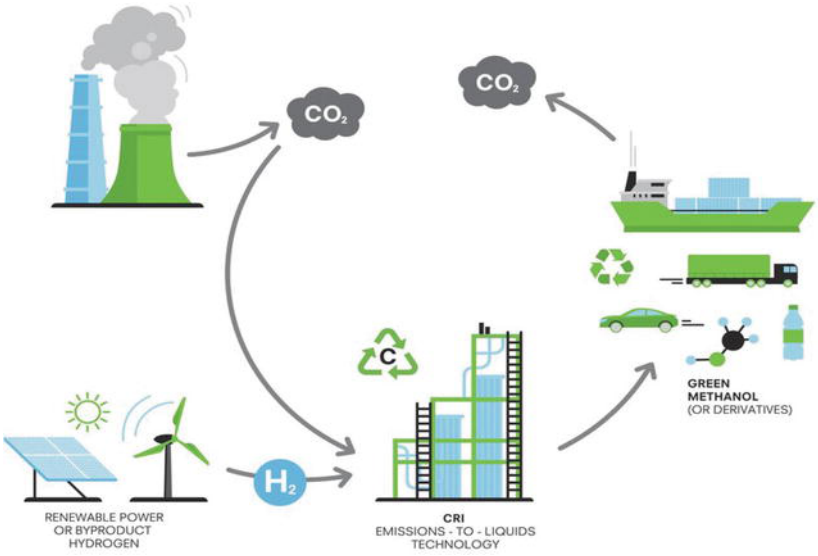

Figure 1.1: Closing the carbon cycle via CO_2 hydrogenation to Methanol[6]

Since 2012, CRI has been producing methanol from CO_2 from waste gas streams and hydrogen from renewable power. The plant has production capacity of 50,000-100,000 ton/year of methanol[7]. A traditional methanol production plant produces 0.7 ton CO_2 per ton methanol from natural gas reforming while more than 3 ton CO_2 per ton methanol based on coal gasification. However, CRI's plant in Iceland consumes 1.3 ton CO_2 per ton of methanol produced from industrial point sources of CO_2 emissions. This demonstrates the potential of the process to be greener and sustainable while tackling the issue of reducing CO_2 concentration in the atmosphere[8].

1.2.3. THERMODYNAMIC ANALYSIS

It should be noted that reaction eqs. (1.1) to (1.3), are linearly dependent and a combination of any two is sufficient to describe the equilibrium mixture. Reactions (1.1) and (1.2) are reversible, exothermic in nature and have less number of gaseous products against reactants. Hence, low temperature and high pressure are favourable to drive the equilibrium towards full conversion. However, low temperature results in slower kinetics of the reactions rendering them incapable for large scale production of methanol.

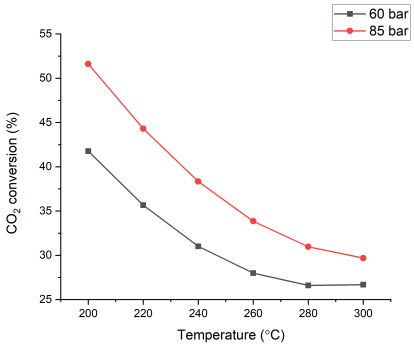

(a) Conversion of CO_2 with pressure variation

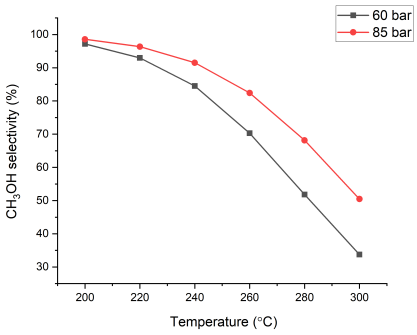

(b) Selectivity of CH_3OH with pressure variation

Figure 1.2: Thermodynamic data at different pressures for CO_2 hydrogenation to methanol [1]. Reaction conditions: P = 60 and 85 bar, Temperature = 200 - 300°C, CO_2:H_2 = 1:3. No CH_4 was considered while performing equilibrium conditions.

From Figure 1.2, it can be seen that at low temperatures (below 200°C) and high pressure, conversion of CO_2 is *ca.* 90% for 85 bar, and 60% for 60 bar. Moreover, selectivity towards Methanol is the highest *ca.* 100% at temperatures below 200°C. This operating condition suffers from being kinetically slow for a considerable conversion to be obtained. It can be said that the conversion is kinetically limited in this temperature range but not thermodynamically.
As we move higher up with temperature from 240 to 300°C, we can observe the conversion of CO_2 staying within a range of 5-10% of each other. This is the temperature range used in the industry for producing Methanol from syngas. Change in kinetics within this temperature range is significant. However, a significant decrease in selectivity is observed. This is because of the competitive RWGS (Reverse Water Gas Shift) Equation 1.3 occurring as a side reaction which is endothermic in nature. Increasing temperature results in more selectivity towards this side reaction consequently forming CO. It can be concluded that at higher temperatures (greater than 240°C), even though kinetics are favourable for greater conversion, a limitation occurs because of thermodynamics of RWGS reaction (1.3) and exothermic nature of CO_2 to methanol (1.2). This push and pull effect/interplay of kinetics and thermodynamics results in a narrow operating window of temperature for direct CO_2 conversion to methanol.

[1] The above data were obtained by using ASPEN Plus v8.8 and SRK equation of state for Equilibrium reactor configuration. This equilibrium data matches the value calculated for 250°C and 50 bar by Gallucci *et al.*[9]

1.2.4. CATALYSTS

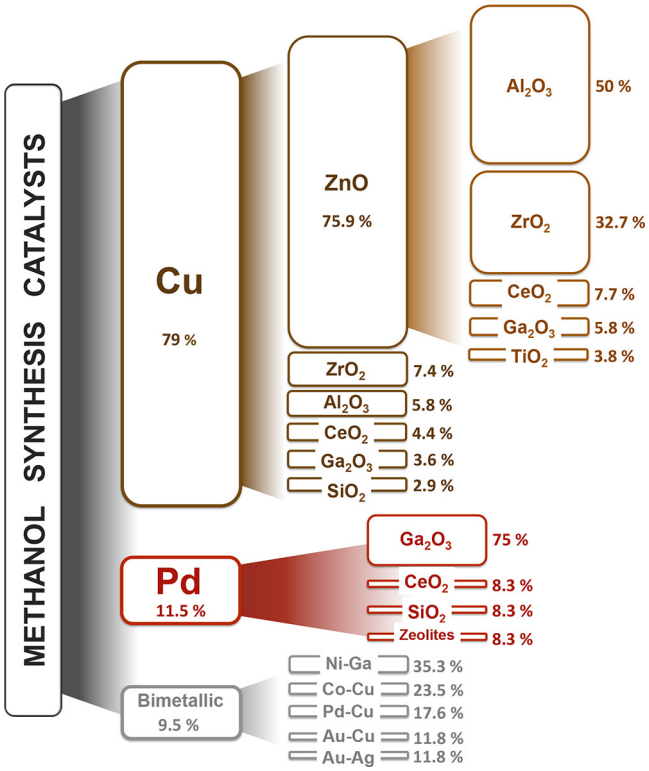

Figure 1.3: Catalysts used for Methanol synthesis[10]

Metals such as Cu, Zn, Cr and Pd are employed to reduce the formation of byproducts such as hydrocarbons and maximise selectivity towards methanol. Metal oxides such as ZnO, ZrO_2, and SiO_2 are widely used as supports. The Cu-ZnO combination of catalysts remains the most widely used for industrial methanol synthesis. These catalysts are prepared via co-precipitation method leading to high Cu loading and dispersion[11]. During this preparation method, formation of aurichalcite ($(Cu_x,Zn_{1-x})_5(CO_3)_2(OH)_6$) mineral is desired. This leads to a highly dispersed Cu^0 metal area when CuO is reduced in the presence of hydrogen[12]. Many authors correlate the activity of Copper-based catalysts to the metallic Cu surface area. Water formed along with methanol as a product of direct CO_2 hydrogenation leads to crystallisation of Cu and ZnO, thereby causing sintering and rapid catalyst deactivation[13].
In recent studies, ZrO_2 has been shown to exhibit good support and promoter characteristics. It shows less hydrophillic character as compared to Al_2O_3, thus inhibiting the sintering effect due to presence of water on the catalyst[14]. The introduction of ZrO_2 leads to formation of strongly basic sites which were shown to be favorable for Methanol selectivity under the work done by Gao *et al.*[15]. Due to this, the Cu-ZnO-ZrO_2 (CZZ) has received significant interest in the catalysis community. Furthermore, the doping effect

1

of Manganese (Mn) on the CZZ system was investigated by Lachowska *et al.*, wherein it was found that the selectivity to methanol was higher than the commercial catalyst[16].

Many authors in the late 20th century have related the activity of catalyst to the surface area of metallic Copper. However, Chinchen *et al.* reported in 1986, that adsorbed Oxygen from CO_2 present in the reaction mixture was responsible for promoting adsorption of CO_2 and H_2 molecules. Unpromoted H_2 adsorption was considered to be fast enough to sustain methanol synthesis[17]. He concluded that only metallic copper sites were responsible for conversion of syngas to methanol and ZnO as a support had no promoting role in the reaction. Several investigations found that Cu^+ might be functioning as the active sites in Methanol synthesis along with metallic Copper. Szanyi *et al.* found that the activity of Cu(100) surface doubled upon oxidation with respect to clean (oxygen-free) Cu(100) surface. The low activity for clean Cu(100) surface was attributed to absence of impurities which help in promotion of ionic Copper concentration[18]. These theories were disputed in the last decade of 20th century, with several authors citing the promotional effects of zinc oxide which are discussed further.

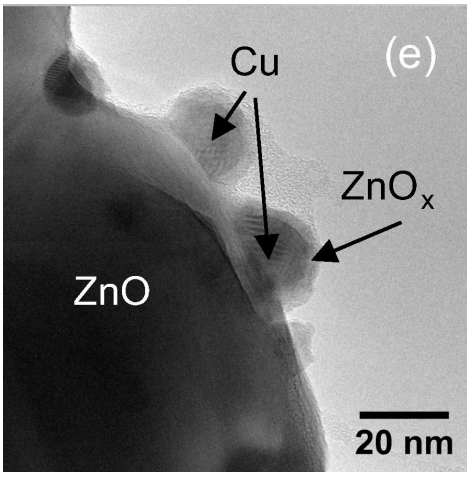

Figure 1.4: Cu ZnO synergy[19]

Apart from the role of metallic and ionic Copper sites, a solid-state interaction between Cu and ZnO results in higher Methanol activity and selectivity. By exposing $CO/CO_2/H_2$ mixture to both Cu/Zn/Al and Cu-ZnO film, Chen *et al.* found that CO is bound to Cu sites while H is bound to ZnO. They concluded that presence of ZnO increased the CO adsorbing capacity of Cu and provided synergistic boost for subsequent hydrogenation to Methanol[20]. Kanai *et al.* proposed the formation of Cu^+-O-Zn species due to migration of ZnO_x over to the copper surface and formation of Cu-Zn alloy. This formation of active species was caused by the synergistic effects of Cu and ZnO[21]. It is a well-established phenomena among the catalyst community that the activity is due to synergistic effects between main catalyst and support or promoter. As explained by Kanai *et al.*[21] and confirmed by Fujitani *et al.*[22], this could be due to transfer of species among different components which could or could not be in direct physical contact.

Since ZrO_2 is less hydrophillic in nature as compared to conventionally used Al_2O_3[14], researchers have tried to take advantage of the synergistic effects of ZrO_2 as a promoter along with ZnO leading to a class of catalysts known as CZZ ($Cu/ZnO/ZrO_2$). Recently

in 2017, Wang *et al.* have demonstrated a very high methanol selectivity (86-91%) and 10% conversion by using a binary ZnO-ZrO_2 solid-state catalyst at operating conditions of 5.0 MPa and 315-320°C with H_2:CO_2 ratio of 3:1 to 4:1. This catalyst demonstrated very high stability results for operation of 500hrs onstream[23]. They concluded strong synergistic effects between ZnO and ZrO_2, because methanol productivity of 13% ZnO-ZrO_2 catalyst (molar basis) was found to be six times of that of mechanically mixed ZnO and ZrO_2. It was also shown recently in 2019 by Wang *et al.*, that similar high conversion and selectivity can be obtained by employing a CZZ catalyst at milder conditions of 3.0 MPa and 220°C[14].

The synergy between Cu and ZrO_2 is mainly attributed to the interfacial Cu-ZrO_2 sites formed. Ro *et al.* found that the turnover frequency was an order of magnitude higher because of these interfacial sites. Further evidence suggested the oxidation states of these sites to be Cu^0 and Zr^{+4}[24]. A physical mixture of Cu-SiO_2 and ZrO_2-SiO_2 did not show an increase in the rate of methanol formation inspired from the work done by Kanai *et al.* to determine similar synergistic effects for ZnO. This suggests that in case of ZrO_2, there is no transfer of species among the catalyst components and indeed, the activity is due to the interfacial sites present. According to Koeppel *et al.*, efficient Cu/ZrO_2 catalysts consist of micro-crystalline Copper particles stabilised through interaction with amorphous ZrO_2 matrix. This configuration resulted in the high interfacial area[25]. Rhodes and Bell in 2005, found that the phases of ZrO_2 have an effect on conversion and selectivity towards Methanol. It was found that Cu/m-ZrO_2 was 10 times more active and exhibited greater selectivity towards Methanol at 3.0 MPa and tempertures between 200 - 250°C for feed of 3 H_2/CO[26]. Samson *et al.* confirmed this phenomena by performing reaction for CO_2 hydrogenation over Cu/ZrO_2 catalysts with varying degree of tetragonal and monoclinic phases of the support. They found an increase in methanol production with increasing content of *t*-ZrO_2[27].

More recently, Magnesium oxide (MgO) has also been explored as a form of support for Cu catalyst. The basicity of MgO enables adsorption of CO_2 on the catalyst and modifies the reaction pathways[28]. Liu *et al.* performed CO_2 hydrogenation over a Cu TiO_2 supported catalyst promoted by MgO. They found that the yield was influenced by the basicity of the surface of catalyst and maximum yield of methanol is obtained at 1% loading of MgO[29].

We can see that focus of catalyst development with regards to CO_2 hydrogenation to methanol has been mostly towards the Cu-ZnO family. In recent years, because of its high activity and the phenomena of Metal-support interaction gaining traction, CZZ class of catalyst is being researched quite significantly. But, there still remains other class of metal oxides such as MgO, CeO_2, TiO_2 which need to be investigated for such interactions.

CATALYST PREPARATION

Out of the different methods for preparing catalysts such as Sol-gel, impregnation (wet and dry), or chemical vapour deposition, co-precipitation method is widely used. Higher

degree of mixing on atomic scale, high metal loading and dispersion can be achieved through this method. Conventionally, metal precursors are mixed with basic precipitating agents such as CO_3^{2-}, HCO_3^- and OH^-. Nitrates are used as metal precursors because of their high solubility. This is followed by heating the mixed solution which causes precipitation of the catalysts in their hydroxide and carbonate form. In case of Cu-ZnO based catalysts, formation of a crystalline zincian malachite and aurachalcite is deemed desirable for highly activity[30]. Precipitation is followed by ageing, drying, calcining and reduction (final step before reaction). Since porosity is created during synthesis in co-precipitation method, control over morphology and texture needs precision[31].
As discussed before, co-precipitation requires a basic precipitating agent and Na_2CO_3 is widely used as one. Using Na_2CO_3 has its own drawbacks. Presence of Na^+ or NO_3^- during calcination results in Cu agglomeration. This decreases final metal dispersion consequently decreasing the catalytic performance[32]. To prevent this, the precipitates (residues) are extensively washed with water to remove Na^+ or NO_3^- before drying. This has led to several authors using other precipitating agents for co-precipitation method. Hong *et al.* reported a $Cu/ZnO/Al_2O_3$ catalyst exhibiting higher metallic copper surface area and high activity prepared via gel-network coprecipitation method. They used a gelatin polymer to form a gel of the metal nitrate solution which was dipped in an oxalic acid solution to obtain precipitates[33]. In another study, Smith *et al.* prepared a co-precipitated Cu/ZnO catalyst using acetate precursor salts and ammonium carbonate as the precipitating agent. It was found that an amorphous zincian georgeite mineral is formed and it shows better performance to a zincian malachite derived catalyst for methanol synthesis from syngas mixture[34].

In this work, we will focus on studying the support and promoter effects of metal oxides such as ZnO, MgO, ZrO_2 and CeO_2 with Cu as active site. Difference between methanol synthesis from CO and CO_2 hydrogenation is also studied. The catalysts will be prepared via co-precipitation method. Urea is chosen as the precipitating agent in this work against the traditionally used Na_2CO_3. This has several advantages:

1. Produces less waste water.
2. No Na^+ ions in the precipitate/residue to wash.
3. More environment friendly.
4. Homogeneous composition of catalyst particles due to slow release of NH_3.

REFERENCES

[1] N. Change, *Carbon dioxide concentration | nasa global climate change,* (2020).

[2] R. G.-M. K. S. K. B. P. N. L. O. V. S. J. A. S. D. C. F. . J. P.-R. Matthias S. Frei, Cecilia Mondelli, *Atomic-scale engineering of indium oxide promotion by palladium for methanol production via co2 hydrogenation,* Nature Communications **10**, 220 (2019).

[3] S. Verhelst, J. W. Turner, L. Sileghem, and J. Vancoillie, *Methanol as a fuel for internal combustion engines,* Progress in Energy and Combustion Science **70**, 43 (2019).

[4] M. Aresta and A. Dibenedetto, *Utilisation of co2 as a chemical feedstock: opportunities and challenges,* Dalton Transactions , 2975 (2007).

[5] S. G. Jadhav, P. D. Vaidya, B. M. Bhanage, and J. B. Joshi, *Catalytic carbon dioxide hydrogenation to methanol: A review of recent studies,* Chemical Engineering Research and Design **92**, 2557 (2014).

[6] S. A. Al-Saydeh and S. J. Zaidi, *Carbon dioxide conversion to methanol: Opportunities and fundamental challenges,* Carbon Dioxide Chemistry, Capture and Oil Recovery 10.5772/intechopen.74779.

[7] *Co2 to methanol plants,* (2020).

[8] C. R. International, *Curbing carbon emissions with green methanol,* (2019).

[9] F. Gallucci, L. Paturzo, and A. Basile, *An experimental study of co2 hydrogenation into methanol involving a zeolite membrane reactor,* Chemical Engineering and Processing: Process Intensification **43**, 1029 (2004).

[10] A. Alvarez, A. Bansode, A. Urakawa, A. V. Bavykina, T. A. Wezendonk, M. Makkee, J. Gascon, and F. Kapteijn, *Challenges in the greener production of formates/formic acid, methanol, and dme by heterogeneously catalyzed co2 hydrogenation processes,* Chemical Reviews **117**, 9804 (2017).

[11] S. M. Kim, M. E. Lee, J. W. Choi, D. J. Suh, and Y.-W. Suh, *Role of zno in cu/zno/al2o3 catalyst for hydrogenolysis of butyl butyrate,* Catalysis Communications **12**, 1328 (2011).

[12] A. Budiman, M. Ridwan, S. M. Kim, J.-W. Choi, C. W. Yoon, J.-M. Ha, D. J. Suh, and Y.-W. Suh, *Design and preparation of high-surface-area cu/zno/al2o3 catalysts using a modified co-precipitation method for the water-gas shift reaction,* Applied Catalysis A: General **462-463**, 220 (2013).

[13] J. Wu, M. Saito, M. Takeuchi, and T. Watanabe, *The stability of cu/zno-based catalysts in methanol synthesis from a co2-rich feed and from a co-rich feed,* Applied Catalysis A: General **218**, 235 (2001).

[14] Y. Wang, S. Kattel, W. Gao, K. Li, P. Liu, J. G. Chen, and H. Wang, *Exploring the ternary interactions in cu/zno/zro2 catalysts for efficient co2 hydrogenation to methanol,* Nature Communications **10** (2019), 10.1038/s41467-019-09072-6.

[15] P. Gao, F. Li, H. Zhan, N. Zhao, F. Xiao, W. Wei, L. Zhong, H. Wang, and Y. Sun, *Influence of zr on the performance of cu/zn/al/zr catalysts via hydrotalcite-like precursors for co2 hydrogenation to methanol,* Journal of Catalysis **298**, 51 (2013).

[16] M. Lachowska and J. Skrzypek, *Methanol synthesis from carbon dioxide and hydrogen over mn-promoted copper/zinc/zirconia catalysts,* Reaction Kinetics and Catalysis Letters **83**, 269 (2004).

[17] G. C. Chinchen, M. S. Spencer, K. C. Waugh, and D. A. Whan, *Promotion of methanol synthesis and the water-gas shift reactions by adsorbed oxygen on supported copper catalysts,* Journal of the Chemical Society, Faraday Transactions 1: Physical Chemistry in Condensed Phases **83**, 2193 (1987).

[18] J. Szanyi and D. W. Goodman, *Methanol synthesis on a cu(100) catalyst,* Catalysis Letters **10**, 383 (1991).

[19] C. Tisseraud, C. Comminges, T. Belin, H. Ahouari, A. Soualah, Y. Pouilloux, and A. Le Valant, *The cuzno synergy in methanol synthesis from co2, part 2: Origin of the methanol and co selectivities explained by experimental studies and a sphere contact quantification model in randomly packed binary mixtures on cuzno coprecipitate catalysts,* Journal of Catalysis **330**, 533 (2015).

[20] H. Chen, S. Lau, L. Chen, J. Lin, C. Huan, K. Tan, and J. Pan, *Synergism between cu and zn sites in cu/zn catalysts for methanol synthesis,* Applied Surface Science **152**, 193 (1999).

[21] Y. Kanai, T. Watanabe, T. Fujitani, T. Uchijima, and J. Nakamura, *The synergy between cu and zno in methanol synthesis catalysts,* Catalysis Letters **38**, 157 (1996).

[22] T. Fujitani and J. Nakamura, *The chemical modification seen in the cu/zno methanol synthesis catalysts,* Applied Catalysis A: General **191**, 111 (2000).

[23] J. Wang, G. Li, Z. Li, C. Tang, Z. Feng, H. An, H. Liu, T. Liu, and C. Li, *A highly selective and stable zno-zro 2 solid solution catalyst for co 2 hydrogenation to methanol,* Science Advances **3**, e1701290 (2017).

[24] I. Ro, Y. Liu, M. R. Ball, D. H. K. Jackson, J. P. Chada, C. Sener, T. F. Kuech, R. J. Madon, G. W. Huber, and J. A. Dumesic, *Role of the cu-zro2 interfacial sites for conversion of ethanol to ethyl acetate and synthesis of methanol from co2 and h2,* ACS Catalysis **6**, 7040 (2016).

[25] R. Koeppel, A. Baiker, and A. Wokaun, *Copper/zirconia catalysts for the synthesis of methanol from carbon dioxide,* Applied Catalysis A: General **84**, 77 (1992).

[26] M. RHODES and A. BELL, *The effects of zirconia morphology on methanol synthesis from co and h2h2 over cu/zro2cu/zro2 catalystspart i. steady-state studies,* Journal of Catalysis **233**, 198 (2005).

[27] K. Samson, M. Sliwa, R. P. Socha, K. Gora-Marek, D. Mucha, D. Rutkowska-Zbik, J.-F. Paul, M. Ruggiero-Mikolajczyk, R. Grabowski, and J. Sloczynski, *Influence of zro2 structure and copper electronic state on activity of cu/zro2 catalysts in methanol synthesis from co2,* ACS Catalysis **4**, 3730 (2014).

[28] V. D. Dasireddy, S. S. Neja, and L. Blaz, *Correlation between synthesis ph, structure and cu/mgo/al2o3 heterogeneous catalyst activity and selectivity in co2 hydrogenation to methanol,* Journal of CO2 Utilization **28**, 189 (2018).

[29] C. Liu, X. Guo, Q. Guo, D. Mao, J. Yu, and G. Lu, *Methanol synthesis from co2 hydrogenation over copper catalysts supported on mgo-modified tio2,* Journal of Molecular Catalysis A: Chemical **425**, 86 (2016).

[30] M. Behrens, F. Girgsdies, A. Trunschke, and R. Schlogl, *Minerals as model compounds for cu/zno catalyst precursors: Structural and thermal properties and ir spectra of mineral and synthetic (zincian) malachite, rosasite and aurichalcite and a catalyst precursor mixture,* European Journal of Inorganic Chemistry **2009**, 1347 (2009).

[31] D. G. M. Prof. Dr. Jacob A. Moulijn, Prof. Freek Kapteijn, *Heterogeneous catalysis for chemical engineers,* DelftChemTech, Section RCE, Delft University of Technology, Julianalaan 136 (2006).

[32] G. Prieto, K. P. de Jong, and P. E. de Jongh, *Towards greener catalyst manufacture: Reduction of wastewater from the preparation of cu/zno/al2o3 methanol synthesis catalysts,* Catalysis Today **215**, 142 (2013).

[33] Z.-s. Hong, Y. Cao, J.-f. Deng, and K.-n. Fan, *Co 2 hydrogenation to methanol over cu/zno/al 2 o 3 catalysts prepared by a novel gel-network-coprecipitation method,* Catalysis letters **82**, 37 (2002).

[34] P. J. Smith, S. A. Kondrat, P. A. Chater, B. R. Yeo, G. M. Shaw, L. Lu, J. K. Bartley, S. H. Taylor, M. S. Spencer, and C. J. e. a. Kiely, *A new class of cu/zno catalysts derived from zincian georgeite precursors prepared by co-precipitation,* Chemical Science **8**, 2436 (2017).

2

EXPERIMENT

2.1. CATALYST SYNTHESIS

For the purpose of catalytic testing, Urea hydrolysis method was used for co-precipitating catalysts. Nitrate precursors of metals were used for this method. The main advantage of this method is no production of waste water into the environment. Conventionally, Sodium carbonate (Na_2CO_3) is used as a precipitating agent. But, using this compound leads to production of waste water because of the washing of Na^+ ions from precipitate. Urea hydrolysis method is slow and the pH is controlled by the release of NH_3 from urea molecules. During hydroysis, OH^- ions are generated from Equation 2.1.

$$CO(NH_2)_2 + H_2O \rightarrow 2NH_4^+ + HCO_3^- + OH^- \tag{2.1}$$

This in turn controls the precipitation rate and ensures that no concentration gradient of precipitants is in the solution[1, 2]. The ratio of Urea used against the nitrate precursors was 4:1. The content of CuO to other metal oxides was maintained around 32 to 40 wt%. All the required chemicals were weighed and dissolved in 500 mL of deionised water. This solution was then transferred to a round bottom flask which was heated at 90°C and stirred continuously for 24 hours.

Table 2.1: Metal precursors used during catalyst synthesis by urea hydrolysis method

Metal	Precursor used	Molar mass of precursor (g/mol)
Cu	$Cu(NO_3)_2.\ 3H_2O$	241.6
Zn	$Zn(NO_3)_2.\ 6H_2O$	297.5
Zr	$ZrO(NO_3)_2.\ xH_2O$	231.23
Mg	$Mg(NO_3)_2.\ 6H_2O$	256.4
Ce	$Ce(NO_3)_2.\ 6H_2O$	434.23

After this, the solution was cooled down to room temperature and vacuum filtered and washed with 500 mL of deionised water. The precipitate was then dried for 12 hours

after which, it was calcined. The calcination was done in a furnace where the dried precipitate was heated at a rate of 2°C/min upto 300°C and maintained for 1 hour at this temperature. The furnace was allowed to cool down to room temperature naturally. After this, the catalyst was pelletised and sieved in size of 90-300 micron.

2.2. CATALYTIC ACTIVITY TESTING

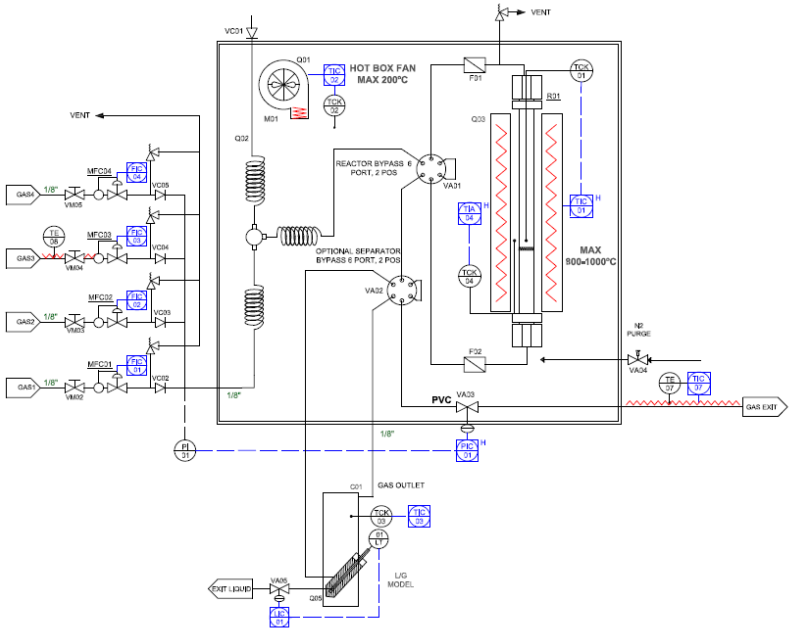

Figure 2.1: Schematic of reactor setup

The experiments were carried out in a quartz glass tube lined Stainless steel reactor with ID of 4 mm. Samples of 200 mg of catalyst (sieve fraction 90-300 microns) diluted with SiC were packed in this reactor. Filters with mesh size of 5 microns were placed upstream and downstream of the reactor to ensure no foreign particles contaminated the reactor. The flow and composition of the inlet gas were controlled by 4 MFCs (Mass flow controllers) with description below.

Table 2.2: Mass flow controllers detailed description

	Gas	Range (mL/min)
MFC-01	N_2	0-300
MFC-02	CO_2/H_2 mixture (30:70)	0-600
MFC-03	CO	0-300
MFC-04	H_2	0-600

The pressure at the inlet of the reactor was controlled by a needle valve PIC-01 located at the downstream of the reactor. Composition of the outlet gas was analysed by a Gas Chromatograph with 3 different channels for detection (Detailed description of the GC provided in Appendix E). All process lines were heated to 120°C to prevent condensation of methanol and water. The gas-liquid separator module was bypassed for all experiments performed.
The catalyst in its oxide precursor state was reduced in a pure H_2 stream at 300°C for 30 minutes under atmospheric pressure. The reactor was then cooled down to room temperature. The system was first pressurised and then heated to the required process conditions. The catalytic activity was determined under the following conditions:

1. For CO_2 hydrogenation to methanol: pressure of 60 and 85 bar (considering 5% N_2 in feed composition, actual total pressure of CO_2 and H_2 was 57 and 80.75 bar respectively), temperature range of 200 - 300°C, GHSV = 24000 1/hr with a stoichiometric ratio of H_2:CO_2 = 3:1.

2. For CO hydrogenation to methanol: pressure of 85 bar (considering 5% N_2 in feed composition, actual total pressure of CO and H_2 was 80.75 bar) , temperature range of 200 - 300°C, GHSV = 24000 1/hr with a stoichiometric ratio of H_2:CO = 2:1.

It should be noted that GHSV stands Gas Hourly Space Velocity which can be thought of as the velocity of the reaction mixture. The higher the GHSV number, higher is the reactant velocity and lower the residence time of reaction mixture in reactor. Technically, GHSV is calculated using the following formula.

$$GHSV = \frac{\text{Volumetric flow of reactant gases}}{\text{Catalyst bed volume}} \tag{2.2}$$

The catalysts were tested for a period of 130 minutes over each temperature value at a 20°increase in step size from 200 until 300°C. It was assumed that there were no transport limitations present in the reactor. A detailed analysis of the same can be found in Appendix C.
CO_2 hydrogenation to methanol The conversion of CO_2 and selectivity to methanol were calculated using the following equations:

$$X_{CO_2} = \frac{F_{CO_{2,in}} - F_{CO_{2,out}}}{F_{CO_{2,in}}} * 100 \tag{2.3}$$

$$S_{MeOH} = \frac{F_{CH_3OH_{out}}}{F_{CH_3OH_{out}} + F_{CO_{out}}} * 100 \tag{2.4}$$

$$S_{CO} = \frac{F_{CO_{out}}}{F_{CH_3OH_{out}} + F_{CO_{out}}} * 100 \tag{2.5}$$

CO hydrogenation to methanol The conversion of CO and selectivity to methanol were calculated using the following equations:

$$X_{CO} = \frac{F_{CO_{in}} - F_{CO_{out}}}{F_{CO_{in}}} * 100 \tag{2.6}$$

$$S_{MeOH} = \frac{F_{CH_3OH_{out}}}{F_{CH_3OH_{out}} + F_{CO_{2,out}}} * 100 \tag{2.7}$$

$$S_{CO_2} = \frac{F_{CO_{2,out}}}{F_{CH_3OH_{out}} + F_{CO_{2,out}}} * 100 \tag{2.8}$$

Although Equation 1.1 suggests CH_3OH being the only molecule formed as a product of CO hydrogenation, formation of CO_2 was noted at higher operating temperatures. Only CH_3OH and CO were detected as the product and by-product respectively of CO_2 hydrogenation. No peaks of CH_4 were detected in the chromatograph in case of either CO or CO_2 hydrogenation.

2.2.1. REACTOR CONFIGURATION

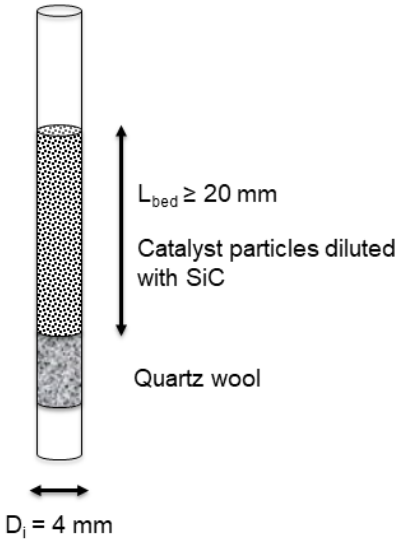

Figure 2.2: Detailed reactor configuration

The mesh size of the particles was chosen such that the ratio of $d_t/d_p > 10$. This was done to ensure negligible wall effects due to inefficiency of packing near the walls[3].
The volume of 200 mg catalyst sample was insufficient for bed height to experience negligible axial dispersion. Hence, dilution of the catalyst bed with SiC particles of 80 micron mesh size was done which is inert to the reactions taking place. This has several positive effects such as:

1. Enhanced heat conduction in the bed.
2. Decreased axial dispersion effects due to a larger bed height.
3. Distribution of the heat generated by exothermic reactions over a larger volume of bed.

Care should be taken to ensure complete homogeneous mixing of the catalyst with the diluent. Otherwise, it may lead to bypassing of the catalyst. As a rule of thumb, the catalyst bed should not be diluted more than 5 to 10 times[4]. A detailed analysis of this

problem in context of the reactor configuration is done in Appendix A on the basis of the work done by van den Beek *et al.*.

2.3. CHARACTERISATION

2.3.1. N_2O TITRATION

The amount of active metallic Copper surface area in the reduced catalysts was determined through reactive adsorption of N_2O at 90°C. The measurements were carried out in a flow reactor made of quartz glass with a length of 20 cm and inner diameter of 6 mm. Catalyst of approximately 300 mg was reduced in the presence of 30mL/min 10% H_2/Ar mixture flow at 300°C over a period of 10 minutes at a ramp rate of 10°C/min. After this, the catalyst was cooled down to 90°C. Then, 150μL of N_2O pulses were injected every 4 minutes until Equation 2.9 was completed. The amount of reacted N_2O, released N_2 were measured using a mass spectrometer (Prisma QMS200 Pfeiffer). It is assumed that reoxidation of the reduced Copper metal sites takes place according to the following reaction.

$$2Cu_{(s)} + N_2O_{(g)} \rightarrow Cu_2O_{(s)} + N_{2(g)} \tag{2.9}$$

The copper surface was calculated based on the assumption that copper crystallites are spherical.

$$S_{Cu} = \frac{\text{moles of} N_2O * SF * N_A}{SD_{Cu} * \text{mass of catalyst}} \tag{2.10}$$

We obtain copper surface area in m^2/g. SF is Stoichiometric factor equal to 2, N_A is Avogadro's number equal to $6.022*10^{23}$ atoms/mol and SD_{Cu} is copper surface density equal to $1.47*10^{19}$ atoms/m^2.

2.3.2. XRD ANALYSIS

The structures of the samples were measured by X-ray diffraction(XRD) using a Bruker D8 Advanced diffractometer with Co Kα source (λ = 0.179 nm). The operations were carried out at 35 kV and 40 mA using Lynxeye position sensitive detector. The samples were measured in the range of 15°<2θ<90°with step mode (A step size of 0.01°and a measuring time of 6s per step were employed).

REFERENCES

[1] I. Atake, K. Nishida, D. Li, T. Shishido, Y. Oumi, T. Sano, and K. Takehira, *Catalytic behavior of ternary cu/zno/al2o3 systems prepared by homogeneous precipitation in water-gas shift reaction,* Journal of Molecular Catalysis A: Chemical **275**, 130 (2007).

[2] T. Shishido, Y. Yamamoto, H. Morioka, K. Takaki, and K. Takehira, *Active cu/zno and cu/zno/al2o3 catalysts prepared by homogeneous precipitation method in steam reforming of methanol,* Applied Catalysis A: General **263**, 249 (2004).

[3] C. F. Chu and K. M. Ng, *Flow in packed tubes with a small tube to particle diameter ratio,* AIChE Journal **35**, 148 (1989).

[4] J. Perez-Ramirez, *The six-flow reactor technology a review on fast catalyst screening and kinetic studies,* Catalysis Today **60**, 93 (2000).

3

RESULTS AND DISCUSSION

3.1. CO_2 HYDROGENATION

3.1.1. EFFECT OF METAL OXIDE PROMOTERS ON CO_2 HYDROGENATION FOR CU-BASED CATALYST

Commercial catalyst ($Cu/ZnO/Al_2O_3$) is chosen as the benchmark catalyst for CO_2 hydrogenation to methanol. First, Cu-ZnO catalyst prepared by Urea hydrolysis is compared against the commercial catalyst ($Cu/ZnO/Al_2O_3$).

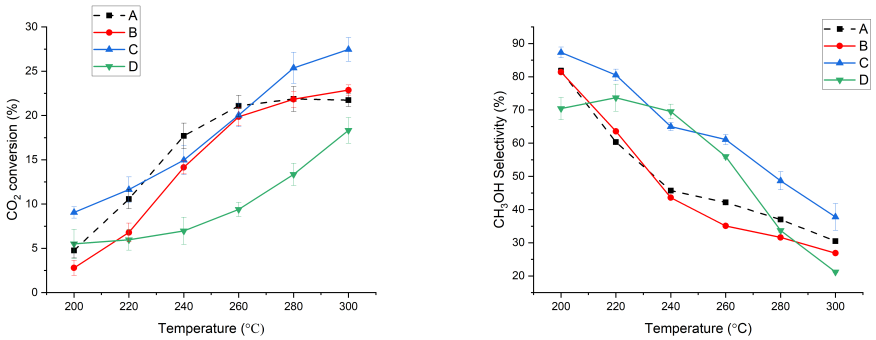

(a) (b)

Figure 3.1: Effect of temperature on 3.1a - CO_2 conversion and 3.1b - Selectivity towards methanol.
Reaction conditions: P = 60 bar, GHSV = 24,000 h^{-1} and CO_2:H_2 = 1:3.
Catalysts used: A : Commercial catalyst ($Cu/ZnO/Al_2O_3$), B : Cu-ZnO, C : Cu-ZrO_2, D : Cu-MgO

As can be seen from Figure 3.1, the conversion increases linearly with temperature upto 260°C and then begins to plateau at a conversion of *ca.* 22%. But, a closer look at the selectivity trend shows a decreasing trend towards methanol suggesting preference for the competing, endothermic RWGS (Equation 1.3) with increasing temperature. Inspite

of higher selectivity (greater than 45%) towards methanol at temperatures below 240°C and favourable thermodynamics, both the commercial and Cu-ZnO catalyst suffer from low conversion, *ca.* 10% and 7% respectively. This shows that the low temperatures, the reaction is under kinetic regime where the conversion of CO_2 is limited by the kinetics. However, at temperatures ranging from 260-300°C, the conversion of CO_2 seems to be flattened and there is no corresponding gain with increase in temperature. On the other hand, selectivity towards methanol also seems unfavourable as it drops from *ca.*45% to 30% with increase in T. In this higher temperature range, thermodynamics has an upper hand over kinetics concerning the selectivity towards formation of CO via RWGS reaction. This can also deduced from the graphs in Figure 1.2a and Figure 1.2b, where the maximum thermodynamic conversion of CO_2 stays relatively constant *ca.* 26-28% in this higher temperature range with a steep drop in the selectivity as we increase temperature. It can be said that there is switch over of regimes from being kinetic limited upto 240°C favouring the selectivity of methanol, while from 260°C onwards the reaction reaches its kinetic potential but is thermodynamically limited due to the favoured RWGS reaction. This is evident from Figure 3.2 below which compares space time yield of methanol for commercial catalyst and Cu-ZrO_2 across the temperature range.

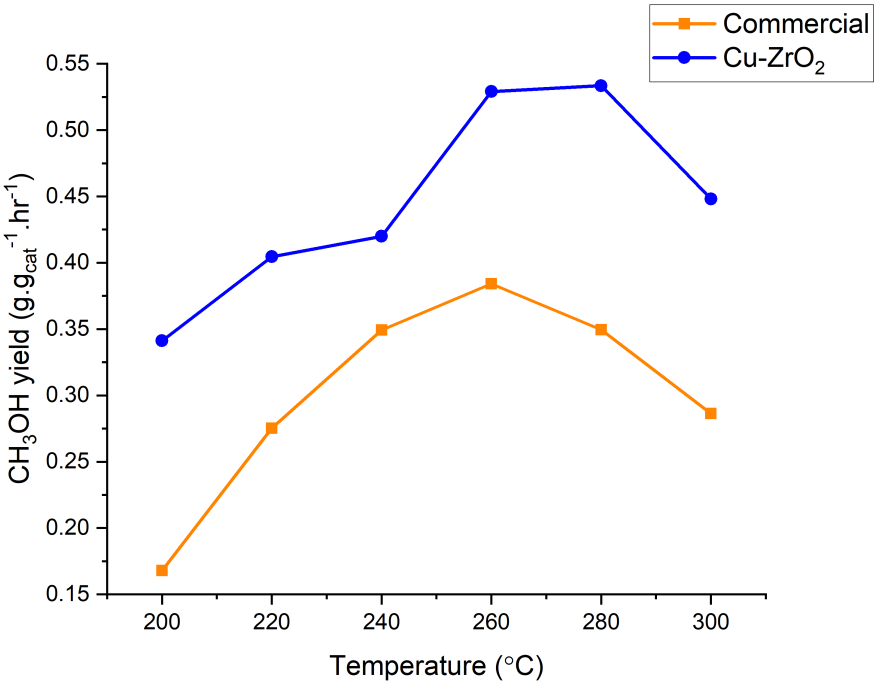

Figure 3.2: Space time yield comparison of commercial catalyst ($Cu/ZnO/Al_2O_3$) vs Cu-ZrO_2. Reaction conditions: P = 60 bar, GHSV = 24,000 hr^{-1}, CO_2:H_2 = 1:3

Another interesting trend is how closely Cu-ZnO follows the commercial catalyst in terms of both selectivity and conversion. This suggests that there is no promotional effect shown by Alumina (Al_2O_3) in CO_2 hydrogenation. This has been proved in the works of Chinchen *et al.* and Sigzek that alumina has no effect on catalytic activity and presents a solid structural framework for the catalyst to resist sintering at the operating conditions[1, 2]. Notably, recently in the early 2000s, Agrell *et al.* affirmed the role of alumina as a structural promoter wherein they studied different Cu-ZnO catalyst systems for Steam reforming of methanol (which is the reverse reaction of CO_2 hydrogenation)[3].

After establishing that alumina does not play a promoting role in the Cu-ZnO catalyst system, we take a look at the other two oxide supports i.e., ZrO_2 and MgO. In terms of conversion, it seems like a tale of two cities, Cu-MgO barely shows an increase in conversion upto 260°C while Cu-ZrO_2 shows a linear increase in conversion with T. Even though the former suffers from low conversion, it shows remarkable selectivity as compared to the benchmark commercial catalyst in the temperature range of 220 - 260°C. As Cu-MgO moves out of the kinetic limited region from 260°C onwards, the selectivity towards methanol plummets down and eventually gets worse than commercial catalyst at 300°C. Cu-ZrO_2 shows an increased selectivity over the whole range of temperature while possessing similar or increased conversion capability.
Even though Cu-ZrO_2 seems to have reached the equilibrium constraints at higher temperatures of 280 and 300°C, 50 percent selectivity towards methanol is not efficient from the point of view of a process engineer. This may lead to increased operating cost for separation of the products downstream. There is still a deviation of *ca.* 10% in maximum achievable selectivity in the temperature range of 200 - 260°C along with deficiency in conversion.

Table 3.1: Cu^0 dispersed area for various oxide supports

Sample	Cu^0 surface area (m^2/g)
Commercial ($Cu/ZnO/Al_2O_3$)	14.4
Cu-ZnO	10.1
Cu-ZrO_2	1.49
Cu-MgO	-
Cu-CeO_2	16.8

Although the commercial and Cu-ZnO catalyst show similar characteristic, they vastly differ in Cu^0 surface area. Surprisingly, Cu-ZrO_2 shows similar conversion and better selectivity towards methanol despite having very low Cu^0 surface area as compared to Cu-ZnO and commercial catalyst as evident from Table 3.1. This shows that there is neither a direct or an inverse correlation between activity and copper metal surface area. There are contradicting evidences in literature regarding this relationship. Chinchen *et al.* showed that the methanol synthesis activity of $Cu/ZnO/Al_2O_3$ obeys a linear relationship with total copper surface area. Their work indicated an identical turn over for all catalysts which included MgO and SiO_2 as supports[4]. However, G*ü*nter *et al.* proposed that structural defects in Cu resulting from ZnO in Cu or incomplete reduction of

ZnO modify the copper surface area, thus, influencing the catalytic activity. Based on results obtained in this work, it can be said that the activity of a Cu-based metal oxide catalyst is not a discrete function of the active metal and support oxide but rather, there exists a synergy between these two functions which helps in CO_2 hydrogenation.
Similar work done by Larmier *et al.* in 2017 with ZrO_2 as support for Cu metal suggests no relationship between methanol synthesis activity and copper surface area. It was observed under *in-situ* IR analysis that neither pure Cu nor ZrO_2 is able to generate methoxy species consequently converted to methanol. Isotope labelling ^{13}C of formate (HCOO*) confirmed its role as a reaction intermediate to produce methoxy species. This indicates the presence of copper-zirconia interface responsible for increased activity [5].

Developing Cu-ZnO-ZrO_2 tertiary catalysts

Based on the results of the previous section, Cu-ZrO_2 is the most promising catalyst. Recently, there has been a shift in focus towards ZrO_2 as a potential support because of its basicity and less hydrophilic nature[6].

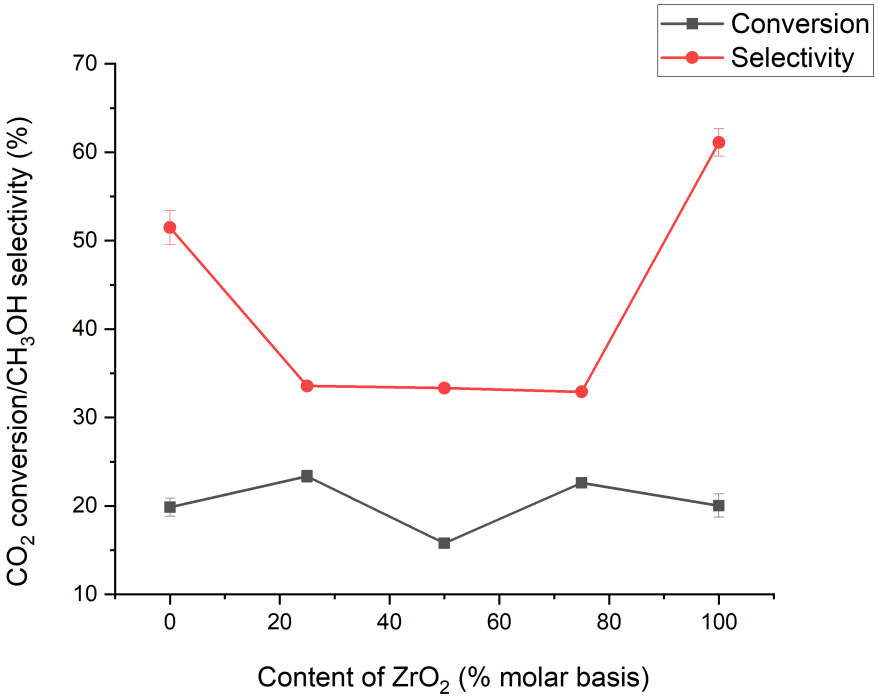

Figure 3.3: Effect of ZrO_2 doping on Cu-ZnO catalyst system.
Reaction conditions: P = 60 bar, Temperature = 260°C, CO_2:H_2 = 1:3

Figure 3.3 indicates general trend observed in regards to conversion and selectivity over the temperature range of 200 - 300°C by varying ZrO_2 molar content. Results for

different operating temperatures from 200 to 300°C can be found in Appendix B. Values on X-axis of 0% indicates Cu-ZnO catalyst while 100% means Cu-ZrO_2 catalyst. There appears to be a minima in selectivity when doping of ZrO_2 is done along with ZnO. A similar minimum in conversion is exhibited, but at an equimolar loading of ZnO:ZrO_2 . However, there is a slight increase in conversion at unequimolar loading of the oxides. Contradicting results in literature show a very strong interaction between ZnO and ZrO_2 boosting both conversion and selectivity towards methanol[6, 7].
Under the work done by Wang J. *et al.*, a ZnO-ZrO_2 solid solution catalyst of 13 molar % Zinc ratio showed exceptional methanol selectivity of 86-91 % with 10% CO_2 conversion[7]. Albeit, in this method $Zr(NO_3)_4.5H_2O$ was used as nitrate precursor for ZrO_2 against $ZrO(NO_3)_2$ used for urea hydrolysis. Differences in catalyst preparation exist in the work done by Wang Y. *et al.*, wherein colloidal crystal templating was used against coprecipitation method used in this work. A Cu-ZnO-ZrO_2 catalyst with high CO_2 conversion (18.2%) and 80.2% methanol selectivity were reported at 220°C and 30 bar[6]. It can be concluded that the catalyst preparation method plays an important role in producing this synergistic effect between the oxides. Further evidence can be found in XRD analysis of the CZZ catalyst family prepared by urea hydrolysis method.

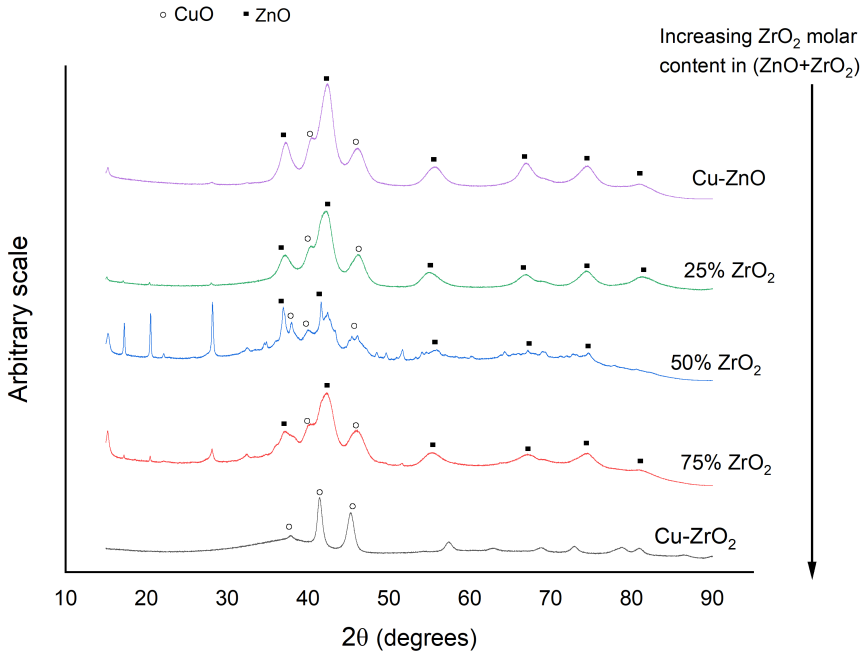

Figure 3.4: XRD analysis of effect of ZrO_2 doping on Cu-ZnO

From the XRD analysis of CZZ catalysts in Figure 3.4, it can be seen that Zirconia is not present in its crystalline form after calcination. However, in the previous work by the two authors, ZrO_2 was detected in its crystalline form (either monoclinic or tetragonal

phase) after calcination. This indicates that the currently used urea hydrolysis method might be incapable of producing a similar synergistic effect. Moreover, work done by Rhodes and Bell in 2005 suggests that pH control during coprecipitation affects crystal structure of the catalyst[8]. Besides the absence of crystalline ZrO_2, the peaks in range of 2θ from 15°to 30°are a worrisome sign. The unmarked peaks at 15°and 17.3°represent Malachite mineral ($Cu_2(CO_3)(OH)_2$)[9], while the one at 28°indicates presence of hydrozincite mineral ($Zn_5(CO_3)_2(OH)_6$)[10, 11]. Presence of these hydroxycarbonate minerals ($(OH)_x(CO_3)_y$) indicates that calcination of the dried residue is not complete. The calcination temperature being 300°C in this work is insufficient for removing CO_3^{-2} and OH^- species from the residue. In Table 3.2 below, we can see the calcination temperatures employed in various works published.

Table 3.2: Calcination temperatures used in literature

Catalyst	Calcination temperature	Method used	Reference
Cu-ZnO-ZrO_2	450°C	Co-precipitation	[6]
Cu-ZnO-Al_2O_3	400°C	Co-precipitation	[12]
Cu-ZrO_2	400/600°C	Co-precipitation	[13]
Cu-ZnO-ZrO_2	350°C	Reverse co-precipitation	[14]
Cu-ZnO-Al_2O_3	350°C	Co-precipitation	[15]
Cu-ZnO	350°C	Urea hydrolysis	[16]

Many works in literature employ a temperature greater than 300°C for calcining the residue. However, using a high temperature for calcination has its own pitfalls. Wang *et al.* in their work studied the evolution of Cu-ZrO_2 catalysts by varying calcination temperature. They used Oxalate Gel-Coprecipitation technique for preparing the catalysts. An increase in crystallite size of CuO while increasing temperature from 350 to 750°C was reported. This was accompanied by a decrease in metallic copper surface area determined by *in-situ* XRD[17]. Although a smaller Cu surface area is undesirable, Wang reported a phase transformation of ZrO_2 taking place at the surface of the catalysts. Highest activity was measured for the catalyst calcined at 550°C which exhibited creation of monoclinic phase over tetragonal phase of ZrO_2. Therefore, there is a trade-off between calcination temperature and dispersed Cu metal area, but, change in crystallinity might help in overcoming this barrier.

Hence, it can be concluded that a better control strategy over pH and tweaks in calcination conditions during catalyst preparation may help in overcoming the amorphous phase of Zirconia and obtain a crystalline structure. This may help in establishing a synergistic effect between the two oxides via urea hydrolysis method.

3.2. GHSV EFFECTS FOR CO_2 HYDROGENATION

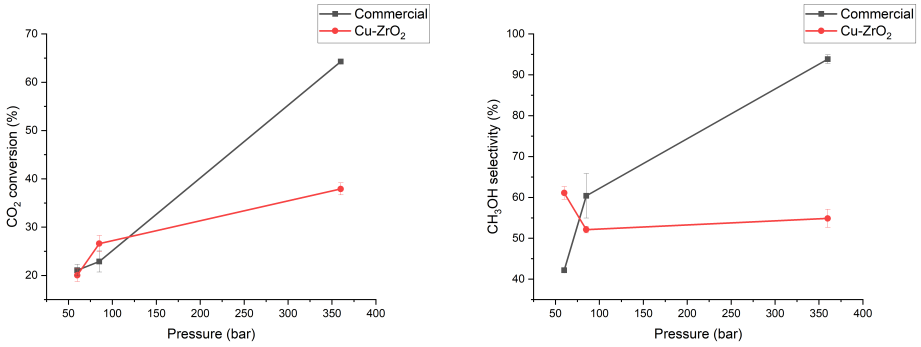

(a) Conversion of CO_2

(b) Selectivity towards methanol

Figure 3.5: Effect of pressure variation on Commercial and Cu-ZrO_2.
Reaction conditions: P = 60, 85 and 360 bar, T = 260°C and CO_2:H_2 = 1:3

As discussed in subsection 1.2.3, thermodynamics dictates that increasing pressure favours both conversion of CO_2 and methanol selectivity. Moreover, from section 3.1, 260°C can be considered as the optimum temperature with respect to space time yield of methanol. Therefore, it was decided to investigate effect of pressure on commercial catalyst and Cu-ZrO_2 at 260°C. From Figure 3.5 both catalysts show an increase in conversion. However, Cu-ZrO_2 surprisingly shows decrease in methanol selectivity with increasing pressure. This increased conversion and selectivity is attributed to *in-situ* condensation of CH_3OH and H_2O formed via Equation 1.2[18]. It is clear from Figure 3.5, that Cu-ZrO_2 is unable to take advantage of this phase change. This can be attributed to the morphology of the catalyst as discussed in Table 3.1.1. Therefore, in order to investigate effects of GHSV on Cu-ZrO_2, pressure of 60 bar seems appropriate.

From the previous discussion we know that maximum space time yield of methanol occurs at 260°C. Hence, a detailed investigation on effects of space velocity at 260°C is done in this work. While referring to Figure 3.1a and Figure 3.7a, it can be said that contribution of CO_2 towards methanol formation upto 260°C is dominant as compared to CO. It can inferred that CO_2 is directly converted to methanol without getting converted to CO and then forming methanol via Equation 1.1. Several authors have regarded CO_2 as the main source of methanol using techniques such as isotope labelling of C and steady state analysis[15, 19]. Considering CO_2 as the main source of methanol, we try to answer the effects of space velocity on conversion and selectivity of Cu-ZrO_2 and commercial catalyst.

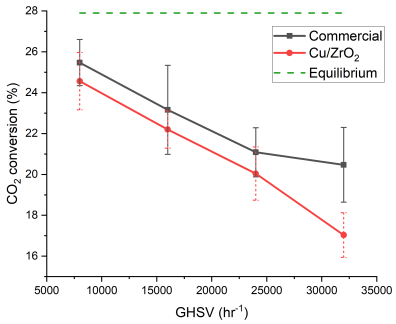

(a) Conversion of CO_2

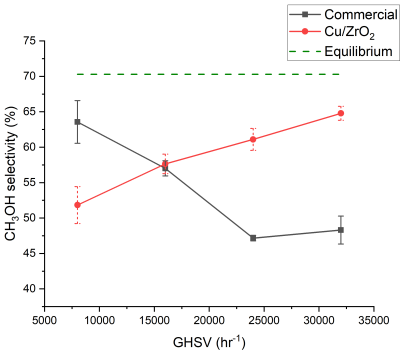

(b) Selectivity towards methanol

Figure 3.6: Effect of GHSV variation on Commercial and Cu-ZrO_2.
Reaction conditions: P = 60 bar, T = 260°C and CO_2:H_2 = 1:3

GHSV was varied from 8000 to 32000 hr^{-1} (equivalent to 60 - 240 $NmL.g_{cat}^{-1}.hr^{-1}$), while mass of catalyst was increased to 600mg without any diluent being used. A drop in CO_2 conversion at high GHSV is observed in Figure 3.6a which favours high external mass transfer. This indicates absence of external mass transfer limitation in the reactor setup in the current configuration. At lower GHSV (longer contact times), clearly both catalysts are reaching thermodynamic limit in terms of conversion as indicated by the dashed green line in Figure 3.6a. However, it is not beneficial to over-reduce GHSV as the catalytic performance becomes worse due to decrease in methanol selectivity exhibited by Cu-ZrO_2 in Figure 3.6b. Decrease in space time yield is observed in case of commercial catalyst deterred by low volumetric and mass flow rates despite showing better conversion and selectivity at lower GHSV.

In section 3.1, we talked about CO_2 hydrogenation being kinetically limited at temperatures below 260°C. This is proved experimentally via conversion of CO_2 at lower GHSV. In case of commercial catalyst at 240°C, the observed CO_2 conversion at GHSV of 24,000 hr^{-1} and 8,000 hr^{-1} remains unchanged at 17%. Usually, decreasing GHSV results in increased residence time of reactants in the reactor and consequently a higher conversion. Although the limit of equilibrium conversion increases from *ca.* 28% at 260°C to *ca.* 33% at 240°C (refer to Figure 1.2a in subsection 1.2.3), observed conversion remains unchanged. Qualitatively, this indicates that temperature below 260°C is not sufficient to overcome the activation energy barrier and increasing reaction rate. Quantitatively, the three-fold decrease of GHSV from 24,000 to 8,000 hr^{-1} does not compensate with any increased conversion of CO_2. Hence, it can be deduced that the current GHSV of 24,000 hr^{-1} is the optimum condition for temperature range of 200 to 300°C. Any decrease would result in lower space time yield, while going higher would result in insignificant conversion observed at temperatures from 200 to 240°C.

Table 3.3: Space time yield comparison at different GHSV for Commercial and Cu-ZrO_2. Reaction conditions: P = 60 bar, Temperature = 260°C, CO_2:H_2 = 1:3

	CH_3OH yield ($g.g_{cat}^{-1}.hr^{-1}$)	
Catalyst / GHSV (hr^{-1})	Commercial	Cu-ZrO_2
8000	0.233	0.183
16000	0.380	0.368
24000	0.402	0.529
32000	0.558	0.635

An interesting aspect of varying GHSV is the increase in space time yield of methanol ($g.g_{cat}^{-1}.hr^{-1}$) with GHSV as seen in Table 3.3. Although both catalysts suffer from low conversion at higher GHSV, high volumetric/mass flow rate of the reactants ensure that the productivity of methanol is greater at conditions far from ideal as compared to equilibrium. Practically, high CO_2 conversion and selectivity may not be the determining factors for performance of a reactor system if the unconverted stream can be recycled efficiently. A classic example is cyclohexane oxidation to cyclohexanol and cyclohexanone with 80% selectivity and 4-8% single pass conversion[20]. An advantage of using higher GHSV is the elimination of external mass transfer limitation and a higher convective heat transfer rate from the catalyst particle to flowing fluid. This reduces the likelihood of hot spots generation within the reactor and consequent deactivation of the catalyst. Several other factors such as energy demand for recycling process should be considered while choosing an optimal GHSV.

Cu-ZrO_2 shows contrasting trend of increasing selectivity towards methanol with GHSV (Figure 3.6b). This indicates either a different reaction pathway of CO_2 hydrogenation or different behaviour of intermediate steps as compared to commercial catalyst.

Without getting into depth with mechanistic aspects of catalytic activity, we will discuss this phenomena. Since it is well established among various authors and evident from the experiments performed that at temperatures of 260°C and below, CO_2 is the main source of methanol. At lower GHSV, there is more contact time between the catalyst and the reactants. This will result in more CO_2 getting adsorbed on the surface and being converted to methanol. This also gives a higher likelihood of sufficient H spillover over the catalyst surface for hydrogenation. There is formation of CO from CO_2 via RWGS because of its thermodynamic favorability at higher temperatures. This trend is followed brilliantly by commercial catalyst.

From Table 3.1, we know that metallic copper surface area is very low in case of Cu-ZrO_2. This metallic site is responsible for Hydrogen dissociation along with CO_2 adsorption on ZrO_2 support sites. The reaction then proceeds via formate pathway which consequently is hydrogenated to methoxy [5]. The hydrogenolysis of formate species (HCOO*) is said to be the rate limiting step[21]. Due to absence of sufficient copper metal sites, this step has less likelihood of taking place. At low GHSV, there will be less spillover of H* than required for hydrogenation and reverse reaction of methanol decomposition to CO and H_2 (reverse of Equation 1.1) might be taking place due to its endothermic nature. As we move up higher in GHSV, there is less contact time for CO_2

and H_2 coadsorption. Moreover, because of high GHSV, the desorption of hydrogenated formate species to methanol is quicker and formate species are adsorbed on the surface for shorter time reducing likelihood of decomposition to CO. This might explain lower conversion and higher selectivity at high GHSV for Cu-ZrO_2.
In order to verify whether this anomaly of increasing selectivity is due to internal mass transfer limitation or not, the reaction was performed using a particle size of 50-90 micron as compared to 90-300 micron at similar pressure and GHSV conditions. It was found that both conversion and selectivity data match within +/- 2% error and are reproducible. Although one might suggest using a particle size of an order of magnitude smaller (10-20 microns), it was observed that using this particle size would result in significant pressure drop in the reactor evident from Figure C.1 in section C.3.

3.3. CO HYDROGENATION

Traditionally, methanol is produced from syngas which is a mixture of CO and CO_2. In this work, we focused on using a pure CO stream because there is exclusivity in production formation (CH_3OH) as against CO_2 hydrogenation. An advantage is the ease of separation (namely, partial condensation) in downstream of the reactor unit.

3.3.1. CATALYTIC ACTIVITY AT 85 BAR

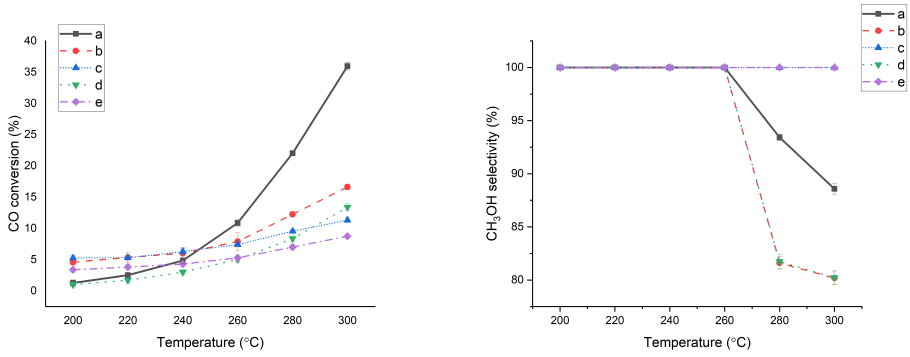

(a) (b)

Figure 3.7: Effect of temperature on 3.7a - CO conversion and 3.7b - Selectivity towards methanol.
Reaction conditions: P = 85 bar, GHSV = 24,000 h^{-1} and CO:H_2 = 1:2.
Catalysts used: a : Commercial catalyst ($Cu/ZnO/Al_2O_3$), b : Cu-ZnO, c : Cu-MgO, d : Cu-ZrO_2, e : Cu-CeO_2

As seen from Figure 3.7a, CO conversion to methanol is similar for all metal oxide supports prepared using urea hydrolysis against commercial catalyst upto 260°C. Although the reaction is favorable thermodynamically at lower temperatures because of its high exothermicity (ΔH_r = -90.5 kJ/mol), the reaction is kinetically limited. We can see a spike in activity of both the commercial and Cu-ZnO catalyst at temperatures > 260°C. The difference in conversion of CO to methanol in case of these two catalysts can be attributed to respective difference in Cu^0 surface area. However, the same cannot be said of the catalyst with other metal oxide support such as CeO_2 which exhibits the lowest conversion among all inspite of having the highest available Cu^0 surface area. Cu-CeO_2 has been reported to be a very good WGS candidate and helps in oxidation of CO to CO_2 [22–25]. Hence, inspite of the high metallic copper surface area, it might not be able to reduce CO to methanol.

Table 3.4: Selectivity towards methanol at higher temperatures for CO hydrogenation. Reaction conditions: P = 85 bar, GHSV = 24,000 hr^{-1} and CO:H_2 = 1:2

Temperature (°C) / Catalyst	280	300
Commercial (Cu/ZnO/Al_2O_3)	93.4	88.6
Cu/ZnO	81.6	80.2
Cu/ZrO_2	81.7	80.2

Although both the commercial and Cu-ZnO catalyst show superior activity towards methanol at higher temperatures of 280 and 300°C, they do produce CO_2 at these temperatures. It should be noted that the other two catalysts, Cu-MgO and Cu-CeO_2 do not suffer from this limitation. At the same time, these two catalysts do not have noticeable increase in activity while increasing temperature. As can be seen from Table 3.4, both Cu-ZnO and Cu-ZrO_2 behave identically with regards to methanol selectivity and produce CO_2 at higher temperatures. Two potential reactions pop up for explaining this phenomena. One being methanol steam reforming (reverse of Equation 1.2) and the other being disproportionation of CO into CO_2 and C (commonly known as Boudouard reaction). Since methanol is being produced from CO hydrogenation, there is no likelihood of water being formed as a product according to Equation 1.1. Hence, the former case is not responsible for CO_2 formation. This suggests that Boudouard reaction, might be taking place at higher temperatures. Since this reaction is highly exothermic in nature, it is favoured at low temperatures[26, 27]. This behaviour is not reported in the literature for Cu-based catalysts in methanol synthesis because of experiments using a either pure CO_2 or mixture of CO and CO_2 and it is difficult to detect CO_2 being produced from CO in a mixture of CO/CO_2. But, a study done by Lee J. *et al.* on hydrogenation of pure CO mixture over a commercial catalyst dating back to 1993 corroborates this finding[15].

In his work, Lee J. *et al.* showed that catalysts have carbon deposited on the surface using X-ray photoelectron spectroscopy (XPS) with CO_2 selectivity upto 10%, operating at temperatures above 290°C. This has a serious implication on operation of Cu-ZnO based catalysts at temperatures beyond 260°C with a pure CO synthesis gas mixture as there will be significant deactivation of the catalyst in its operating cycle. Moreover, all of the catalysts including commercial suffer from very low single pass conversion, *ca.* 10% upto 260°C. There is a spike in conversion of CO beyond this temperature limit. Therefore, one faces a dilemma when operating with a syngas feed of pure CO. Should one operate within the limitations of temperature and suffer from lower conversion and yield or risk deactivating the catalyst and consequently frequent maintenance of the reactor.

However, this limitation can be overcome by taking advantage of either MgO or CeO_2 in conjunction with ZnO for supporting Cu catalyst. A similar approach was taken in this work by preparing an equimolar support of MgO and ZnO (MgO:ZnO = 1:1) and CO hydrogenation was done at identical reaction conditions. This data can be found in detail in Figure 3.8a. There seems to be a synergistic effect between the two oxides as conversion of CO to methanol indeed improves than using the two oxides (MgO and ZnO)

individually. Another interesting thing to note is that though addition of ZnO helps in improving conversion of CO, the selectivity is maintained at 100%. This indicates that there is no CO_2 formation and hence, no coking or deactivation of the catalyst at higher temperatures while using MgO as a promoter/support for CO hydrogenation.

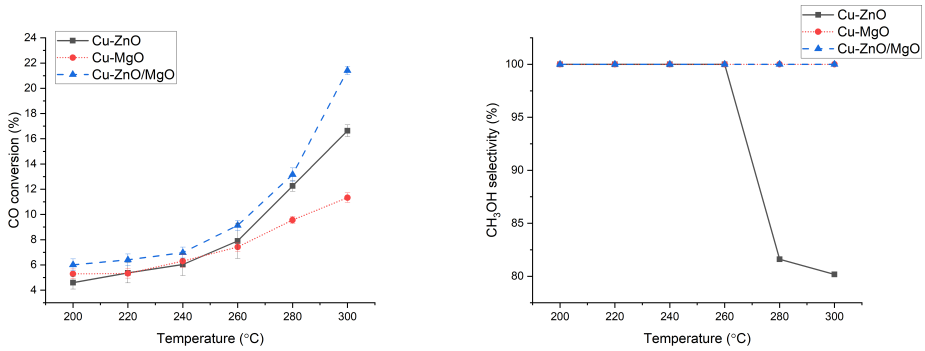

(a) Conversion of CO

(b) Selectivity towards methanol

Figure 3.8: Synergy of ZnO and MgO for CO hydrogenation.
Reaction conditions: P = 60 bar, GHSV = 24,000 hr^{-1} and CO:H_2 = 1:2

3.4. NOVEL CONFIGURATION FOR CO_2 HYDROGENATION

3.4.1. CURIOUS CASE OF CU-CERIA

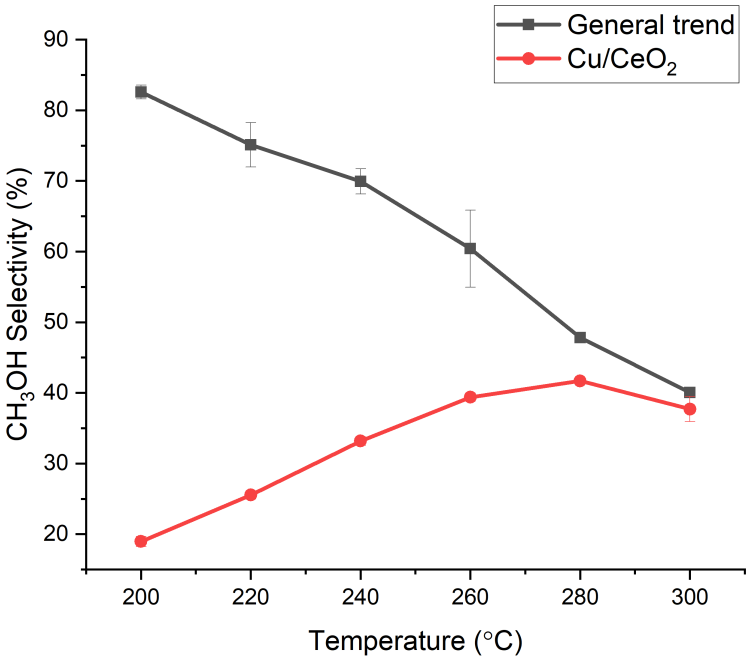

Figure 3.9: Selectivity to methanol for Cu-CeO_2 for CO_2 hydrogenation. Reaction conditions: P = 85 bar, GHSV = 24,000 hr^{-1} and CO_2:H_2 = 1:3

As can be seen from Figure 3.9, methanol selectivity of Cu-CeO_2 is very low and follows an opposite trend as compared to other Cu based metal oxide catalysts. Although recent works show Cu-CeO_2 being more selective than Cu-ZrO_2[28] and formation of Cu-Ceria interface favourable for direct CO_2 hydrogenation not seen on Cu-Zn alloy[29]. There is contradicting evidence suggesting that Cu-CeO_2 favours water gas shift reaction than CO_2 hydrogenation[22–25], which corroborates the findings of this work.

3.4.2. NOVEL CONFIGURATION FOR INCREASING SELECTIVITY

As discussed previously, a high percentage of CO_2 converted by Cu-Ceria catalyst goes to CO rather than CH_3OH. Since it is well established that the main source of methanol is CO_2 rather than CO, RWGS (Equation 1.3) is considered as a side reaction and CO a by-product of the main CO_2 hydrogenation reaction. Treating CO_2 hydrogenation to methanol as a two step reaction involving conversion of CO_2 to CO via RWGS and the subsequent conversion of CO to methanol has its advantages. This indirect hydrogenation has been pioneered under the alias of CAMERE (carbon dioxide hydrogenation to

methanol via reverse water gas shift reaction) process[30]. A pilot plant based on this process is operated by the Korean Institute of Energy and Research (KIER) and Korea Gas Corporation (KOGAS)[31]. A part of the feedstock containing mixture of CO_2 and H_2 is first sent to RWGS reactor. Water from the reactor effluent stream is separated from the stream and the syngas mixture of $CO/CO_2/H_2$ is then sent to the second reactor. Modelling results show an increase in methanol productivity via CAMERE process[30].

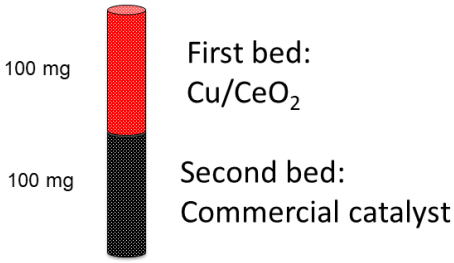

Figure 3.10: Dual bed configuration

Taking inspiration from CAMERE's configuration, Cu/CeO_2 was placed as the first bed promoting RWGS reaction and then $Cu/ZnO/Al_2O_3$ (Commercial catalyst) promoting methanol synthesis from syngas mixture instead of direct CO_2 hydrogenation. The difference between CAMERE and dual bed configuration in this work is:

1. Single reactor instead of two.
2. Similar operating conditions for RWGS and methanol synthesis from syngas.
3. No fresh feed of pure hydrogen to maintain composition of syngas.

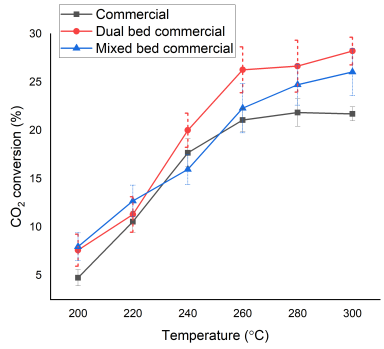

(a) Conversion of CO_2

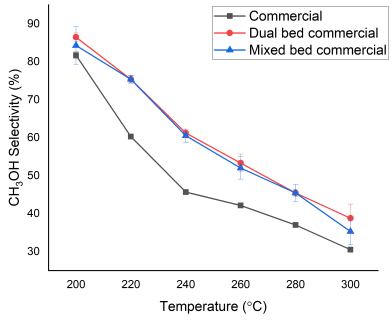

(b) Selectivity towards methanol

Figure 3.11: Comparison of Commercial (200 mg) vs. dual and mixed configuration of Cu-CeO_2 (100 mg) and commercial catalyst (100 mg). Reaction conditions: P = 60 bar, GHSV = 24,000 hr^{-1} and CO_2:H_2 = 1:3

It can be seen from Figure 3.11, that dual bed configuration shows an improvement in conversion and selectivity to methanol over a commercial catalyst. Although this configuration is advantageous in terms of improved selectivity and methanol yield, it has its own drawbacks. Firstly, the first bed utilises conversion of CO_2 to CO via RWGS reaction, which is endothermic in nature. While the second bed converts the syngas mixture to

methanol, this reaction is exothermic in nature. Despite the fact that dual bed configuration can be used in a single reactor as demonstrated in this work, these two zones need different controlling action to maintain isothermicity on an industrial scale. This makes designing a reactor with this configuration a little difficult. One possible way to circumvent this problem is to employ a mixed bed configuration, wherein Cu-CeO_2 and commercial catalyst are physically mixed.

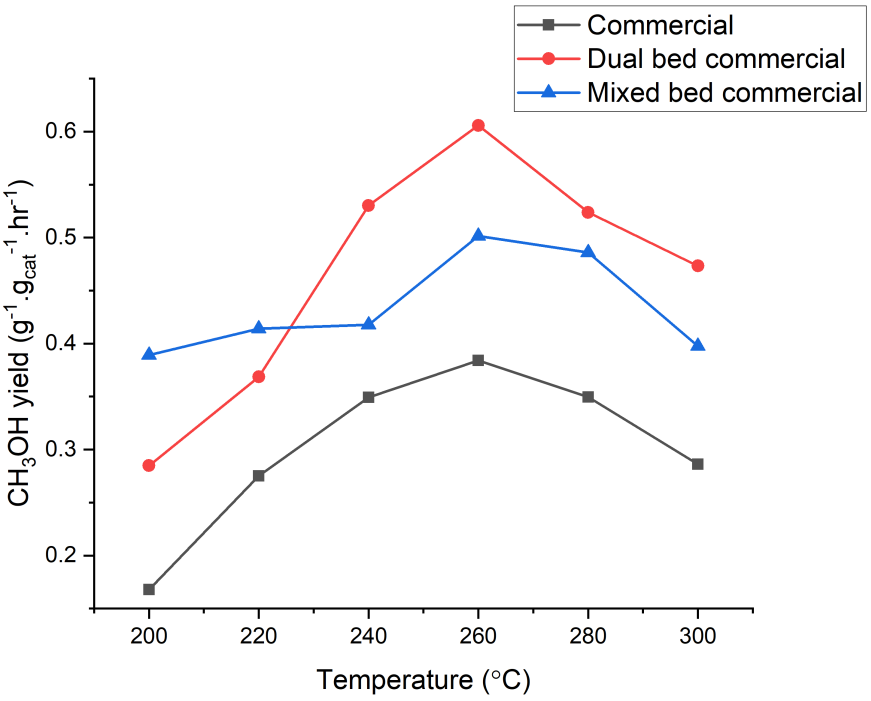

Figure 3.12: Weight time yield comparison of Commercial (200 mg) vs. dual and mixed bed configuration of Cu-CeO_2 (100 mg) and commercial catalyst (100 mg).
Reaction conditions: P = 60 bar, GHSV = 24,000 hr^{-1} and CO_2:H_2 = 1:3

Mixed bed configuration behaves in a similar fashion to dual (sequential) bed exhibiting excellent selectivity towards methanol, however with a lower CO_2 conversion. However, looking at Figure 3.12, provides us with two different perspectives of using either a sequential (dual bed) or mixed bed configuration. Both the configurations show better methanol yield at respective temperatures. At optimum temperature of 260°C, sequential bed shows 58% increase while mixed bed shows 30% increase in methanol yield. This demonstrates an efficient use of the catalyst and reactor volume. Moreover, the mixed bed configuration has a better methanol yield even at low temperature of 200°C as against 260°C for commercial catalyst. This can enable a shift towards low temperature methanol synthesis and has a huge impact on the energy requirement of the pro-

cess. As we move towards low temperature synthesis, less energy is required to heat up the incoming reactants and this reduces the energy required. Besides this, the methanol selectivity of mixed bed configuration at 200°C is *ca.* 84% and this consequently can help to reduce separation costs of the process. Hence, these two configurations open up two different pathways to achieve a more efficient methanol production from CO_2.

As evident from previous discussion, the possibilities presented by sequential bed and mixed bed configuration are immense. Now, we will try to simplify the idea of using these configurations into simple components. The basis of this idea is founded on data already available in literature. One of the hypothesis is that by ensuring RWGS takes place on Cu/CeO_2, the active sites on commercial catalyst are utilised only for direct CO_2 and CO hydrogenation to methanol. Under the work done by Sahibzada *et al.*, it was shown that water plays a promoting effect by altering the adsorbed oxygen coverage on catalyst which in turn helps in increased CO_2 adsorption[32]. Due to presence of $Cu\text{-}CeO_2$, the partial pressure of H_2O and CO is increased via RWGS (Equation 1.3) along with water formed due to direct CO_2 hydrogenation (Equation 1.2). This increased presence of water leads to increase in adsorbed oxygen (O*). The CO generated by RWGS reaction then has the ability to scavenge the adsorbed oxygen and form surface CO_2 species to undergo hydrogenation[33]. This ability of CO can be verified through increase in methanol selectivity of catalysts showing activity for both CO and CO_2 hydrogenation (Appendix D). As shown by Kunkes *et al.*, addition of CO in pure CO_2 stream helps in overcoming the equilibrium yield[34].

Another plausible theory not from a molecular standpoint is that when RWGS reaction takes place on $Cu\text{-}CeO_2$ catalyst, only one molecule of H_2 per CO_2 is consumed. This indeed leads to a slight increase in the hydrogen partial pressure leading a stoichiometric imbalance with respect to CO_2 locally in the reactor. This local increase in partial pressure of hydrogen can explain the increase in selectivity towards methanol as evident from previous studies showing increasing selectivity with increase in H_2:CO_2 ratio[35, 36].

Although it seems counter-intuitive to let the RWGS reaction take place, which is a side reaction of CO_2 hydrogenation and promote formation of by-products; experiments, literature data and validation of methanol synthesis from syngas mixture corroborate this idea of mixed bed configuration and indicates that CO helps in boosting the conversion and selectivity towards methanol. Similar to the work done by Kanai *et al.* in 1996, wherein a physical mixture of Cu/SiO_2 and ZnO/SiO_2 [37] led to establishment of synergy between Cu and ZnO, we could propose a similar synergy effect between CeO_2 and ZnO. Further work would be needed to confirm this. Through this novel configuration and ability of breaking down CO_2 hydrogenation into two tandem (sequential) reactions having opposite exergonic nature within the same reactor to improve selectivity may indeed open up new possibilities.

REFERENCES

[1] G. Sizgek, H. Curry-Hyde, and M. Wainwright, *Methanol synthesis over copper and zno promoted copper surfaces,* Applied Catalysis A: General **115**, 15 (1994).

[2] G. Chinchen, P. Denny, J. Jennings, M. Spencer, and K. Waugh, *Synthesis of methanol,* Applied Catalysis **36**, 1 (1988).

[3] J. Agrell, *Production of hydrogen from methanol over cu/zno catalysts promoted by zro2 and al2o3,* Journal of Catalysis **219**, 389 (2003).

[4] G. Chinchen, K. Waugh, and D. Whan, *The activity and state of the copper surface in methanol synthesis catalysts,* Applied Catalysis **25**, 101 (1986).

[5] K. Larmier, W.-C. Liao, S. Tada, E. Lam, R. Verel, A. Bansode, A. Urakawa, A. Comas-Vives, and C. Copret, *Co2-to-methanol hydrogenation on zirconia-supported copper nanoparticles: Reaction intermediates and the role of the metal-support interface,* Angewandte Chemie International Edition **56**, 2318 (2017).

[6] Y. Wang, S. Kattel, W. Gao, K. Li, P. Liu, J. G. Chen, and H. Wang, *Exploring the ternary interactions in cu/zno/zro2 catalysts for efficient co2 hydrogenation to methanol,* Nature Communications **10** (2019), 10.1038/s41467-019-09072-6.

[7] J. Wang, G. Li, Z. Li, C. Tang, Z. Feng, H. An, H. Liu, T. Liu, and C. Li, *A highly selective and stable zno-zro 2 solid solution catalyst for co 2 hydrogenation to methanol,* Science Advances **3**, e1701290 (2017).

[8] M. RHODES and A. BELL, *The effects of zirconia morphology on methanol synthesis from co and h2h2 over cu/zro2cu/zro2 catalystspart i. steady-state studies,* Journal of Catalysis **233**, 198 (2005).

[9] (2020).

[10] T. Alhawi, M. Rehan, D. York, and X. Lai, *Hydrothermal synthesis of zinc carbonate hydroxide nanoparticles,* Procedia Engineering **102**, 356 (2015).

[11] S. Cherepanova, D. Markovskaya, and E. Kozlova, *Identification of a deleterious phase in photocatalyst based on cd1 - xznxs/zn(oh)2by simulated xrd patterns,* Acta Crystallographica Section B Structural Science, Crystal Engineering and Materials **73**, 360 (2017).

[12] G. Prieto, K. P. de Jong, and P. E. de Jongh, *Towards greener catalyst manufacture: Reduction of wastewater from the preparation of cu/zno/al2o3 methanol synthesis catalysts,* Catalysis Today **215**, 142 (2013).

[13] T. Witoon, J. Chalorngtham, P. Dumrongbunditkul, M. Chareonpanich, and J. Limtrakul, *Co 2 hydrogenation to methanol over cu/zro 2 catalysts: Effects of zirconia phases,* Chemical Engineering Journal **293**, 327 (2016).

[14] F. Arena, G. Italiano, K. Barbera, S. Bordiga, G. Bonura, L. Spadaro, and F. Frusteri, *Solid-state interactions, adsorption sites and functionality of cu-zno/zro2 catalysts in the co2 hydrogenation to ch3oh,* Applied Catalysis A: General **350**, 16 (2008).

[15] J. Lee, K. Lee, S. Lee, and Y. Kim, *A comparative study of methanol synthesis from co2/h2 and co/h2 over a cu/zno/al2o3 catalyst,* Journal of Catalysis **144**, 414 (1993).

[16] R. Fan, M. Kyodo, L. Tan, X. Peng, G. Yang, Y. Yoneyama, R. Yang, Q. Zhang, and N. Tsubaki, *Preparation and application of cu/zno catalyst by urea hydrolysis method for low-temperature methanol synthesis from syngas,* Fuel Processing Technology **167**, 69 (2017).

[17] L.-C. Wang, Q. Liu, M. Chen, Y.-M. Liu, Y. Cao, He, and K.-N. Fan, *Structural evolution and catalytic properties of nanostructured cu/zro2catalysts prepared by oxalate gel-coprecipitation technique,* The Journal of Physical Chemistry C **111**, 16549 (2007).

[18] R. Gaikwad, A. Bansode, and A. Urakawa, *High-pressure advantages in stoichiometric hydrogenation of carbon dioxide to methanol,* Journal of Catalysis **343**, 127 (2016).

[19] G. Chinchen, P. Denny, D. Parker, M. Spencer, and D. Whan, *Mechanism of methanol synthesis from co2/co/h2 mixtures over copper/zinc oxide/alumina catalysts: use of14c-labelled reactants,* Applied Catalysis **30**, 333 (1987).

[20] Y.-J. Xu, P. Landon, D. Enache, A. F. Carley, M. W. Roberts, and G. J. Hutchings, *Selective conversion of cyclohexane to cyclohexanol and cyclohexanone using a gold catalyst under mild conditions,* Catalysis Letters **101**, 175 (2005).

[21] H. Nakatsuji and Z.-M. Hu, *Mechanism of methanol synthesis on cu(100) and zn/cu(100) surfaces: Comparative dipped adcluster model study,* International Journal of Quantum Chemistry **77**, 341 (2000).

[22] Y. Li, Q. Fu, and M. Flytzani-Stephanopoulos, *Low-temperature water-gas shift reaction over cu- and ni-loaded cerium oxide catalysts,* Applied Catalysis B: Environmental **27**, 179 (2000).

[23] L. Barrio, M. Estrella, G. Zhou, W. Wen, J. C. Hanson, A. B. Hungria, A. Hornes, M. Fernandez-Garcia, A. Martinez-Arias, and J. A. Rodriguez, *Unraveling the active site in copper-ceria systems for the water-gas shift reaction: In situ characterization of an inverse powder ceo2-x/cuo-cu catalyst,* The Journal of Physical Chemistry C **114**, 3580 (2010).

[24] H. Yan, C. Yang, W.-P. Shao, L.-H. Cai, W.-W. Wang, Z. Jin, and C.-J. Jia, *Construction of stabilized bulk-nano interfaces for highly promoted inverse ceo2/cu catalyst,* Nature Communications **10** (2019), 10.1038/s41467-019-11407-2.

[25] P. GUNAWARDANA, H. LEE, and D. KIM, *Performance of copper-ceria catalysts for water gas shift reaction in medium temperature range,* International Journal of Hydrogen Energy **34**, 1336 (2009).

[26] J. Hunt, A. Ferrari, A. Lita, M. Crosswhite, B. Ashley, and A. E. Stiegman, *Microwave-specific enhancement of the carboncarbon dioxide (boudouard) reaction,* The Journal of Physical Chemistry C **117**, 26871 (2013).

[27] T. M. (contributor to BioEnergy Discussion Lists), *Boudouard equilibrium,* (2020).

[28] W. Wang, Z. Qu, L. Song, and Q. Fu, *Co2 hydrogenation to methanol over cu/ceo2 and cu/zro2 catalysts: Tuning methanol selectivity via metal-support interaction,* Journal of Energy Chemistry **40**, 22 (2020).

[29] J. Graciani, K. Mudiyanselage, F. Xu, A. E. Baber, J. Evans, S. D. Senanayake, D. J. Stacchiola, P. Liu, J. Hrbek, and J. F. e. a. Sanz, *Highly active copper-ceria and copper-ceria-titania catalysts for methanol synthesis from co2,* Science **345**, 546 (2014).

[30] F. Samimi, D. Karimipourfard, and M. R. Rahimpour, *Green methanol synthesis process from carbon dioxide via reverse water gas shift reaction in a membrane reactor,* Chemical Engineering Research and Design **140**, 44 (2018).

[31] I. Dimitriou, P. Garca-Gutirrez, R. H. Elder, R. M. Cullar-Franca, A. Azapagic, and R. W. K. Allen, *Carbon dioxide utilisation for production of transport fuels: process and economic analysis,* Energy Environmental Science **8**, 1775 (2015).

[32] M. Sahibzada, I. Metcalfe, and D. Chadwick, *Methanol synthesis from co/co2/h2over cu/zno/al2o3at differential and finite conversions,* Journal of Catalysis **174**, 111 (1998).

[33] X.-M. Liu, G. Q. Lu, Z.-F. Yan, and J. Beltramini, *Recent advances in catalysts for methanol synthesis via hydrogenation of co and co2,* Industrial Engineering Chemistry Research **42**, 6518 (2003).

[34] E. Kunkes and M. Behrens, *Methanol chemistry,* (2020).

[35] A. Alvarez, A. Bansode, A. Urakawa, A. V. Bavykina, T. A. Wezendonk, M. Makkee, J. Gascon, and F. Kapteijn, *Challenges in the greener production of formates/formic acid, methanol, and dme by heterogeneously catalyzed co2 hydrogenation processes,* Chemical Reviews **117**, 9804 (2017).

[36] A. U. Atul Bansode, *Towards full one-pass conversion of carbon dioxide to methanol and methanol-derived products,* Journal of Catalysis , 66 (2013).

[37] Y. Kanai, T. Watanabe, T. Fujitani, T. Uchijima, and J. Nakamura, *The synergy between cu and zno in methanol synthesis catalysts,* Catalysis Letters **38**, 157 (1996).

4

CONCLUSION

Methanol synthesis from CO and CO_2 show similar behaviour upto 260°C at high pressure. However, the former still suffers from kinetic limitation upto a certain extent, the latter is limited by thermodynamics. ZnO and ZrO_2 show similar trend as supports in case of CO hydrogenation, while the latter shows exceptional selectivity and conversion in case of CO_2 hydrogenation. However, different methanol selectivity trend of ZrO_2 indicates possibility of a different mechanism. This demands further investigation of the support using *in-situ* IR spectroscopy. The anomalous behaviour of Cu-ZrO_2 showing higher selectivity towards methanol at higher GHSV has a potential application in processes requiring higher throughput with lower conversion.
Magnesium oxide (MgO) shows excellent selectivity towards methanol in case of both CO and CO_2 hydrogenation, albeit showing poor conversion. Higher selectivity makes it a potential candidate to be used in processes where efficient separation and recycling is possible. However, when used in conjunction with ZnO, it shows excellent synergy for CO hydrogenation overcoming the pitfalls of individual oxides.

The use of either a mixed or sequential bed configuration combining a RWGS catalyst and catalyst active for CO/CO_2 hydrogenation indicates improved conversion and selectivity. The sequential bed configuration exhibits *ca.* 50% increases in methanol yield at temperatures greater than 260°C, while mixed bed shows methanol yield better than commercial catalyst even at temperature as low as 200°C at identical space velocity and pressure condition. Although there is an established theory in literature for explaining the phenomena, an experimental and theoretical approach in proving it is required. This can be done by performing either steady state or *in-situ* spatial resolution of the reactor. Theoretically, one can perform phase and chemical equilibrium analysis along the length of reactor using simulator such as ASPEN Plus. There is broad practical scope of mixed bed configuration. One can vary the composition of the two catalysts and get the optimum value for maximum methanol yield. Moreover, a new class of core-shell catalysts with the outer shell promoting RWGS while the inner core comprising of catalyst promoting methanol synthesis from CO/CO_2 can take birth. This can help imitate

the phenomena taking place on the reactor scale (m to mm scale) on a particle scale (microscale), thereby intensifying the process.
Apart from a catalyst design point of view, process parameter such as CO_2:H_2 ratio can be increased greater than stoichiometry. Although researchers might argue that increasing H_2 will result in increased operational (recycling and separation) costs. However, in current scenario too, there is a need for separation and recycling of streams as 100% conversion is not achieved. There is evidence in literature of increased conversion and selectivity by increasing hydrogen content. Increasing operating pressure of the mixed bed or sequential bed can help achieve higher methanol yield. High pressure methanol synthesis has already been demonstrated in previous works of the research group. Methanol selectivity and CO_2 conversion show an absolute deviation of *ca.* 10-12% at 260°C at high pressure of 184 bar. This showcases an opportunity for improvement. Besides this, novel configurations such as membrane reactors can help drive forward equilibrium position converting more CO_2 selectively to methanol. Theoretical models of such reactors do show their superiority. However, the design of catalysts on the membrane pose difficulties in their practical implementation. A series of membrane reactor wherein the reaction mixture from the outlet of reactor is passed over a membrane separating the products and enters the next reactor and so on, is a simplified version. This takes advantage of the high pressure conditions for separation over membrane.
Although we have shown an improvement in methanol synthesis via catalyst preparation and change in bed configuration, there still exists a multitude of options to be explored in order to make the methanol synthesis more efficient.

ACKNOWLEDGEMENTS

I would like to offer my sincere gratitude to my supervisor Prof. dr. Atsushi Urakawa, for his continuous support in shaping and advising me during this work. I am grateful for him giving me enough freedom to explore whilst providing insights to deepen my understanding of the subject. Besides my supervisor, I would like to thank my daily supervisor, Nat Phongpreuksathat (Ph.D candidate) for his patience, support and enthusiasm. With him beside me in building 67, no two days were ever the same as he pushed me for improvement. Apart from the daily scientific research done in the lab, he made sure to have a light-hearted moment and kept my spirits up during my entire thesis journey. I would like to thank my thesis committee members, Prof. dr. Bernard Dam (MECS group, Chemical engineering) and Prof. dr. Wiebren de Jong (Large-scale energy storage, 3mE) for their suggestions and evaluation of my thesis.
I believe that the scientific work carried out in our labs is not possible without the help of non-academic staff involved. I sincerely thank Harrie Jansma and Atul Bansode (Area supervisor and Deputy Area supervisor respectively) of building 67 for their continuous help in troubleshooting my reactor setup. I would like to thank Bart van der Linden, Willy Rook, Xiaohui Liu, Ben Norder and Liliana Baron for their help in characterisation and lab support. I thank my friends here in TU Delft for the stimulating discussions and fun we had during the group assignments. Nothing less to take away from my friends back in India, who helped in taking the journey to TU Delft. Special thanks to my colleagues here in Career center at TU Delft for providing me an exciting opportunity to work alongside and making my journey at the university special.

Finally and above all, I would like to thank my parents and my brother, for their continued support and belief. They encouraged me to follow my dreams and have been a source of inspiration throughout my life. This journey would not have been possible if not for them and I dedicate this work to them.

A

BED DILUTION

In this section, we will discuss whether the particle size being used is within the constraints of bed dilution based on the work done by van den Bleek *et al.* [1]. For an inert bed fraction b and a 5% maximum deviation from ideality, the criteria imposed on particle size is

$$\frac{2.5bd_p}{(1-b)L_b} < 0.05 \tag{A.1}$$

In our case, inert bed fraction b is calculated as

$$b = \frac{\text{mass of inert particle (SiC)}}{\text{mass of total bed}} = \frac{300mg}{500mg} \tag{A.2}$$

Hence, the inert bed fraction is 0.6, while the bed length L_b was found to be 32mm or 0.032m. The particle diameter varied from 90 - 300 micron or $9*10^{-5}$m to $3*10^{-4}$m. Substituting these values in the equation (A.1) for particle diameter of 90 micron, we get bed dilution of 0.0105. Similarly, we get a value of 0.035 for particle diameter of 300 micron. Both of these values fall below 0.05 and satisfy the bed dilution criteria for 5 percent deviation from ideality. Alternatively, one could look up the graph below as reported by Ramirez J. *et al.* which is a graphical representation of the equation[2].

A

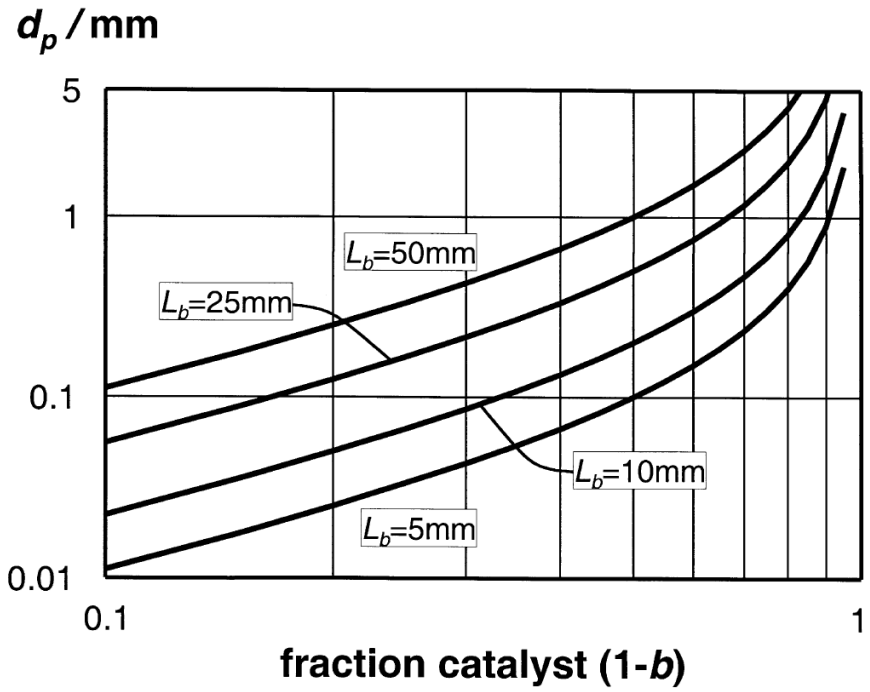

Figure A.1: Bed dilution limits on particle size

B

ZnO-Zirconia synergy

Excluding the lower temperatures of 200 and 220°C wherein all Cu based catalysts are kinetically limited, a pattern in CO_2 conversion and methanol selectivity emerges. With an equimolar ratio of ZnO:ZrO_2 both selectivity and conversion are at minimum. Usinf either of the pure metal oxides as support is beneficial while using urea hydrolysis method for preparing catalyst. As discussed in 3.1.1, varying calcination temperature and other parameters during catalyst preparation might help. The following figures show the catalytic activity at different temperatures for different ZnO:ZrO_2 molar ratios.

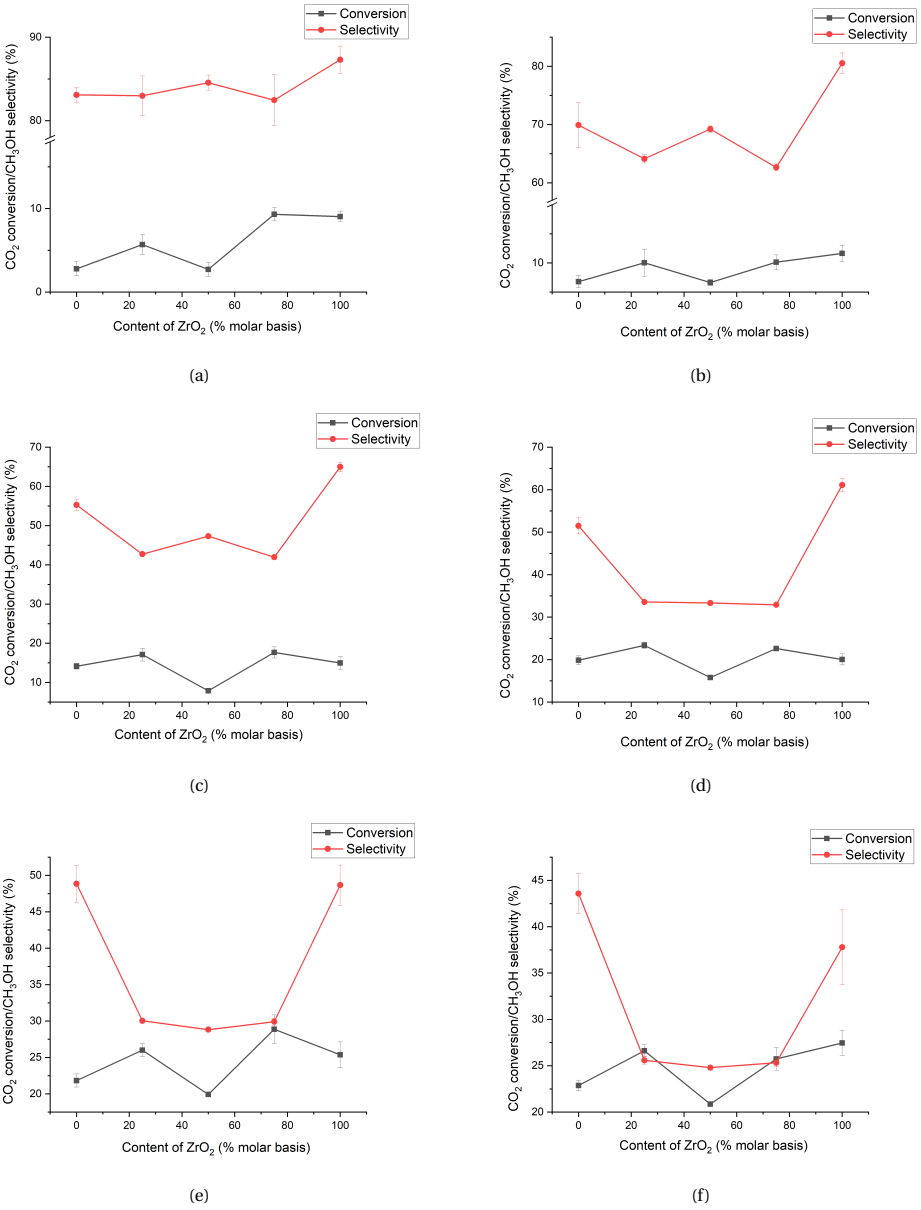

Figure B.1: Effect of Zirconia doping with ZnO for CO_2 hydrogenation at different temperatures. (a) - 200°C, (b) - 220°C, (c) - 240°C, (d) - 260°C, (e) - 280°C and (f) - 300°C.
Reaction conditions: P = 60 bar, GHSV = 24,000 hr^{-1} and CO_2:H_2 = 1:3

C

TRANSPORT PROPERTIES IN REACTOR SETUP

C.1. WALL EFFECTS

The minimum reactor diameter to neglect wall effects in gas-solid operations is

$$\frac{d_t}{d_p} > 10 \tag{C.1}$$

The inner diameter of the quartz tube is 4mm or $4*10^{-3}$m, while the maximum particle diameter is 300 microns or $3.5*10^{-4}$m. This gives the ratio of d_t:d_p equal to 11.4 > 10. Decreasing the catalyst size will increase this ratio. Hence, wall effects can be neglected in the setup.

C.2. AXIAL DISPERSION

Minimum bed length of reactor to neglect axial dispersion is

$$\frac{L_b}{d_p} > \frac{20n}{Bo} ln\left(\frac{1}{1-x}\right) \tag{C.2}$$

L_b is length of bed, d_p is particle diameter, n is order of reaction, Bo is Bodenstein number (also known as particle Peclet number) and x is conversion. Bodenstein number is given by Equation C.3

$$Bo = \frac{u\, d_p}{D} \tag{C.3}$$

Here, u is superficial gas velocity, d_p is particle diameter and D is molecular diffusion coefficient. Superficial gas velocity in the reactor is $7.96*10^{-2}$m/s. Diffusion coefficient of CO_2 at normal conditions is $1.39*10^{-5}$ m^2/s[3]. Diffusion coefficient for gases obeys the

following relation to temperature and pressure according to Maxwell-Boltzmann distribution.

$$D \propto \frac{T^{1.75}}{P} \tag{C.4}$$

According to Equation C.4, the diffusion coefficient for CO_2 at 260°C and 60 bar is 1.0*10^{-6} m^2/s. Maximum conversion attained during experiments for CO_2 was 25% or 0.25 and the reaction is assumed to be of second order. Substituting these values in Equation C.2, we get length of bed should be greater than 1.4*10^{-4} m or 0.14 mm. This condition too is satisfied.

C.3. PRESSURE DROP

The hydrodynamic pressure drop inside the reactor was calculated using Ergun equation.

$$\frac{-\Delta P}{\Delta z} = \frac{150\mu_g(1-\epsilon)^2}{d_p^2\epsilon^3}u + \frac{1.75\rho_g(1-\epsilon)}{d_p\epsilon^3}u^2 \tag{C.5}$$

ϵ is bed void fraction, μ_g is fluid viscosity in Pa.s, d_p is the particle size in metres, ρ_g is density of fluid density in kg/m^3 and u is superficial fluid velocity in m/s.
Δz can be expressed in the form of weight change of catalyst along the bed as:

$$\Delta z = \frac{\Delta w}{A(1-\epsilon)\rho_{cat}} \tag{C.6}$$

w is weight of catalyst in kg, A is cross sectional area of the reactor in m^2. Ergun equation was transformed from reactor length dependence to variation along the catalyst weight as follows:

$$\frac{-\Delta P}{\Delta w} = \frac{150\mu_g(1-\epsilon)}{d_p^2\epsilon^3 A\rho_{cat}}u + \frac{1.75\rho_g(1-\epsilon)}{d_p\epsilon^3 A\rho_{cat}}u^2 \tag{C.7}$$

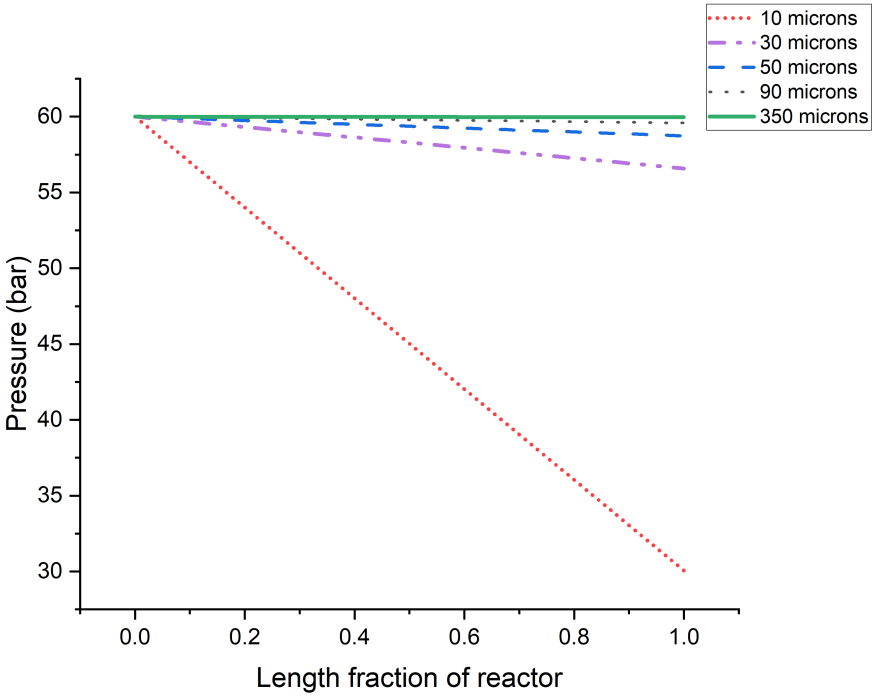

Figure C.1: Pressure drop for CO_2 hydrogenation at 60 bar and GHSV = 24,000 hr^{-1}

C.4. EXTERNAL MASS TRANSFER

As evident from section 3.2, conversion of CO_2 decreases with increasing GHSV. This indicates absence of any external mass transfer limitation. Increase in GHSV means increase in superficial gas velocity. This results in increased mass transfer coefficient (k_g). However, we see a decrease in conversion meaning that inherent reaction rate decreases. This indicates that mass transfer is not limiting and the transport of reactants is reaction controlled.

C.5. INTERNAL MASS TRANSFER

The reactor was used in the same configuration for both CO and CO_2 hydrogenation. But, the former is less complex to model and is more exothermic. Moreover, as we exceed 260°C, the rate of CO and CO_2 hydrogenation become similar. Hence, it was decided to model CO hydrogenation kinetics on the basis of simplicity for both internal mass transfer (Diffusion inside catalyst) and temperature gradient along the length of reactor.
Catalyst effectiveness is checked by computing Thiele modulus which is effectively the ratio of reaction and diffusion within the catalyst particle. Thiele modulus [4] is calcu-

lated as

$$M_T = \frac{(-r'''_{As})\,L}{\left[2D_e \int_{C_{Ae}}^{C_{As}} (-r'''_A) dC_A\right]^{1/2}} \tag{C.8}$$

The reaction rate -r'''_A is based on volume of catalyst pellets. Since we have rate based on mass of catalyst, we can transform the Thiele modulus using mass based rate expression. This can be expressed as

$$M_T = \frac{(-r''_{As})\,L}{\rho_{cat}\left[\frac{2D_e\,\rho_{cat}}{RT} \int_{C_{Ae}}^{C_{As}} (-r''_A) dP_A\right]^{1/2}} \tag{C.9}$$

In Equation C.9, -r_A" is based on mass of catalyst and has units of mol CO consumed. kg^{-1}_{cat}. hr^{-1}.

The reaction rate is calculated using the following equation based on work done by Kuczynski *et al.*[5].

$$R_{CO} = \frac{2.68 * 10^9\, exp(-18400/T)(P_{CO}P^2_{H2} - P_M/K_{eq})}{\left(1 + 0.069P_{CO} + 6.19 * 10^{-8}\, exp(6610/T)P_{H2}\right)^3} \tag{C.10}$$

In this equation P_{CO}, P_{H2} and P_M denote partial pressure of CO, H_2 and methanol respectively in bar. T is absolute temperature in Kelvin scale and K_{eq} is expressed as follows:

$$lnK_{eq} = -28.9762 + 11815/T \tag{C.11}$$

Diffusion coefficient was calculated assuming Knudsen diffusion inside the catalyst pores. Diffusion coefficients were found to be 2.8*10^{-7} and 4.9*10^{-7} for H_2 and CO respectively. Tortuosity and porosity factors were neglected while calculating diffusion coefficient. Since reaction involves both hydrogen and carbon monoxide, the diffusion coefficient of H_2 was used because it is smaller in magnitude, meaning H_2 will diffuse slowly as compared to CO. On substituting respective values in Equation C.9, we obtain Thiele modulus = 0.03. Assuming that the catalyst particles are spherical in shape, effectiveness factor is calculated using the following equation.

$$\eta = \frac{1}{M_T}\left(\frac{1}{tanh\,3M_T} - \frac{1}{3M_T}\right) \tag{C.12}$$

On substituting Thiele modulus, we get an effectiveness factor of 99.9% or approximately 1. Hence, the catalyst does not have any mass transfer limitation. Another method of checking mass transfer limitation is via Weisz-Prater criterion. It is calculated using the following equation[6]

$$C_{WP} = \frac{-(r'_A)_{obs}\,\rho_c\,R^2}{D_e\,C_{As}} \tag{C.13}$$

All terms in Equation C.13 are known or can be measured. -r_A' has units 'mol. kg^{-1}_{cat}.hr^{-1}, R is radius of catalyst particle. C_{As} is surface concentration and is assumed to be equal to bulk concentration. This assumption is valid as it is already proven that there exists no external mass transfer resistance via experiment. The concentration of CO is obtained

via ASPEN Plus. The density of catalyst along with bed porosity was found to be 1400 kg/m^3. Assuming a bed porosity of 0.3, actual catalyst density can be approximated to be 2000 kg/m^3. Substituting these values in Equation C.13, we get

$$C_{WP} = \frac{8.75 * 10^{-4} * 2000 * (300 * 10^{-6})^2}{2.8 * 10^{-7} * 0.5} \frac{mol.kg_{cat}^{-1}.s^{-1}\, kg_{cat}.m^{-3}\, m^2}{m^2.s^{-1}\, kmol.m^{-3}} \tag{C.14}$$

$$C_{WP} = \frac{8.75 * 10^{-4} * 2000 * (300 * 10^{-6})^2}{2.8 * 10^{-7} * 0.5 * 1000} \frac{mol.kg_{cat}^{-1}.s^{-1}\, kg_{cat}.m^{-3}\, m^2}{m^2.s^{-1}\, mol.m^{-3}} \tag{C.15}$$

This gives C_{WP} equal to 1.1*10^{-3} « 1. Hence, there are no concentration gradients within the particle according to Weisz-Prater criterion in Fogler's Elements of Chemical reaction engineering[6].

C.6. INTRA-PARTICLE TEMPERATURE GRADIENT

Thermal gradient within a particle is given by[4]

$$\Delta T_{particle} = \frac{D_e \left(C_{As} - C_{A,centre}\right) (-\Delta H_r)}{k_{eff}} \tag{C.16}$$

C_{As} and $C_{A,centre}$ are concentrations at the surface and centre of catalyst respectively in mol.m^{-3}. -ΔH_r is heat of reaction in J.mol^{-1} and k_{eff} is effective thermal conductivity of the pellet. The concentration of the reactant is unknown but can be calculated using the mole balance of species A over the catalyst particle as follows

$$\frac{2D_A}{r}\frac{dC_A}{dr} + D_A\frac{d^2C_A}{dr^2} = rate \tag{C.17}$$

with boundary conditions C = C_{bulk} at r = R and dC_A/dr = 0 at r = 0. Solving this, we get a concentration profile in terms of partial pressure of CO as shown in Figure C.2. Translating the difference in mole fraction to difference in concentration over the particle, we get ΔC equal to 1 mol.m^{-3}. Effective thermal conductivity is assumed to be 4 W/(m.K) based on the work done by Dimov for Cu based catalysts in 2007[7]. Substituting the respective values in Equation C.16, we get $\Delta T_{particle}$ equal to 0.01°C. Hence, the catalyst particle can be treated to be isothermal.

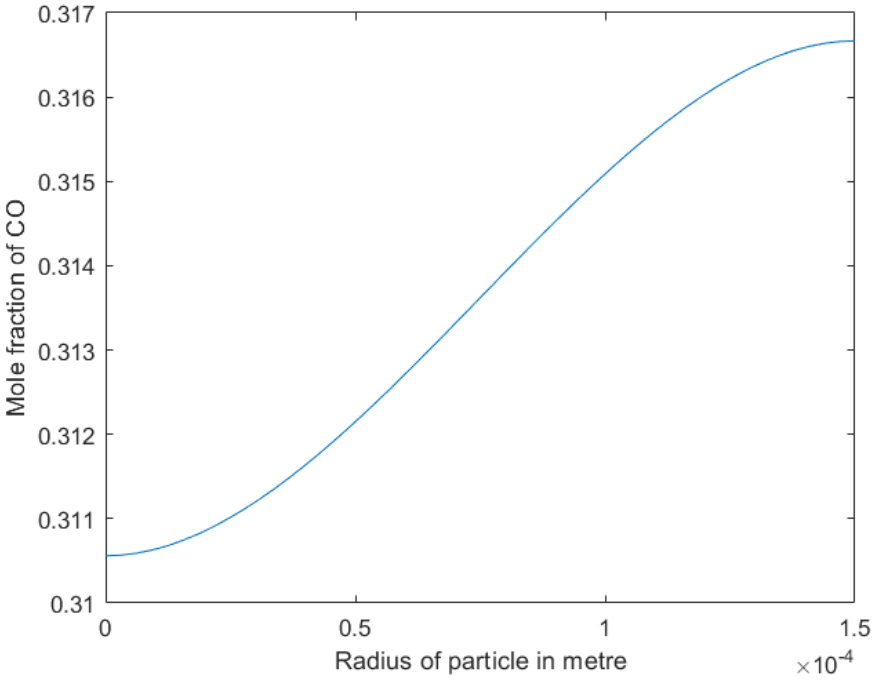

Figure C.2: Mole fraction profile of CO within the catalyst of 300 μm diameter. Reaction conditions: P = 85 bar, T = 280°C, GHSV = 24,000 hr^{-1} and CO:H_2 = 1:2

D

SEQUENTIAL BED CONFIGURATION

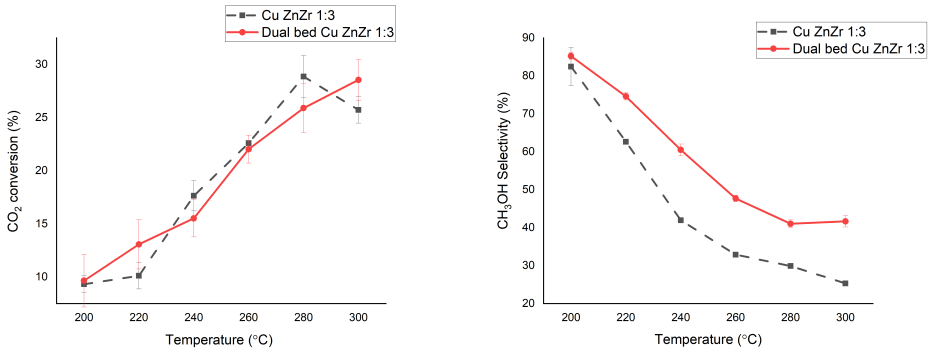

(a) Conversion of CO

(b) Selectivity towards methanol

Figure D.1: Sequential bed configuration of Cu-CeO_2 (100 mg) and Cu ZnO ZrO_2 with molar ratio of ZnO:ZrO_2 = 1:3 (100 mg) vs.Cu ZnO ZrO_2 with molar ratio of ZnO:ZrO_2 = 1:3 (200 mg) for CO_2 hydrogenation. Reaction conditions: P = 60 bar, GHSV = 24,000 hr^{-1} and CO_2:H_2 = 1:3

The molar ratio of ZnO to ZrO_2 used is 1:3 while CuO content in the catalyst is *ca.* 35 wt%.

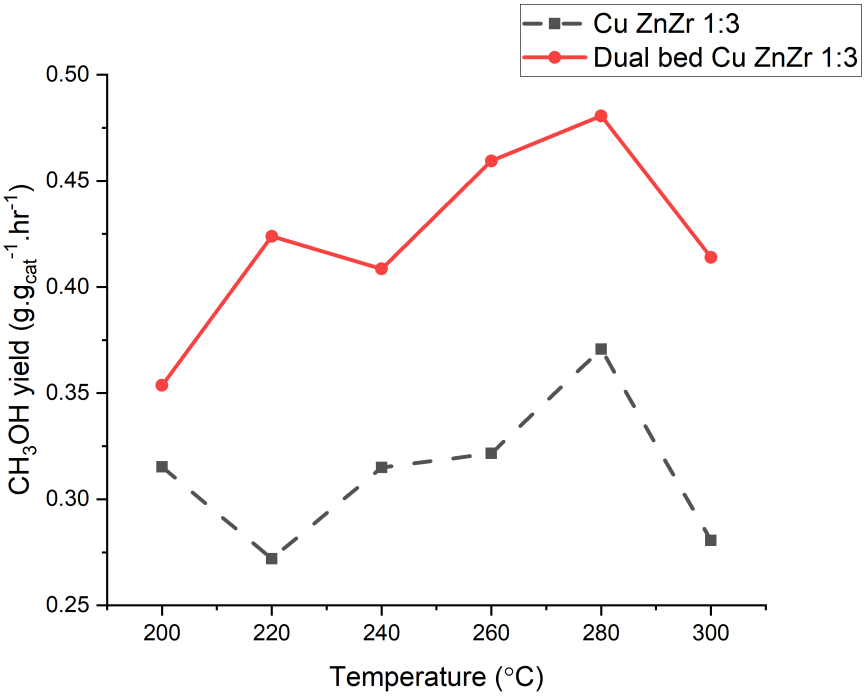

Figure D.2: Weight time yield of Sequential bed configuration of Cu-CeO_2 (100 mg) and Cu ZnO ZrO_2 with molar ratio of ZnO:ZrO_2 = 1:3 (100 mg) vs.Cu ZnO ZrO_2 with molar ratio of ZnO:ZrO_2 = 1:3 (200 mg) for CO_2 hydrogenation.
Reaction conditions: P = 60 bar, GHSV = 24,000 hr^{-1} and CO_2:H_2 = 1:3

E

GAS CHROMATOGRAPH

Reactor outlet gas from the setup was injected in Gas Chromatograph (compact GC Interscience) at an interval of 3 minutes. The GC is equipped with three channels, two thermal conductivity detectors (TCD) and one flame ionisation detector (FID). Details are as follows:

Table E.1: Details of Interscience compact GC

Detector	Gases detected	Pre-column	Oven temperature
FID	Methanol, ethane, propane, butane	Rt-U bond (10m*0.32mm) and Rt-Q bond (14m*0.32mm)	110°C
TCD	CO_2, ethane, propane, H_2O	Rt-Q bond (3m*0.32mm) and Rt-Q bond (10m*0.32mm)	60°C
TCD	H_2, O_2, N_2, CO, Methane	RT-Q bond (4m*0.32mm) and Molsieve $5A^0$ (8m*0.32mm)	50°C

REFERENCES

[1] C. Van Den Bleek, K. Van Der Wiele, and P. Van Den Berg, *The effect of dilution on the degree of conversion in fixed bed catalytic reactors,* Chemical Engineering Science **24**, 681 (1969).

[2] J. Perez-Ramirez, *The six-flow reactor technology a review on fast catalyst screening and kinetic studies,* Catalysis Today **60**, 93 (2000).

[3] D. T. PRITCHARD and J. A. CURRIE, *Diffusion of coefficients of carbon dioxide, nitrous oxide, ethylene and ethane in air and their measurement,* Journal of Soil Science **33**, 175 (1982).

[4] O. Levenspiel, *Chemical reaction engineering* (Wiley India, 2007).

[5] M. Kuczynski, W. Browne, H. Fontein, and K. Westerterp, *Reaction kinetics for the synthesis of methanol from co and h2 on a copper catalyst,* Chemical Engineering and Processing: Process Intensification **21**, 179 (1987).

[6] H. S. FOGLER, *Elements of chemical reaction engineering* (PRENTICE HALL, 2019).

[7] S. V. Dimov, A. G. Sipatrov, N. A. Rudina, V. V. Kuznetsov, and A. A. Khassin, *Thermal conductivity of composite catalysts containing metallic copper as a reinforcing component,* Theoretical Foundations of Chemical Engineering **41**, 184 (2007).

LIST OF FIGURES

E

LIST OF TABLES